January 2014

Satellite Derived Volumetric Soil Moisture In A HEC-HMS Model

Damon Grabow

SATELLITE DERIVED VOLUMETRIC SOIL MOISTURE IN A HEC-HMS MODEL

by

Damon Grabow

A Thesis

Submitted to the Graduate Faculty

of the

University of North Dakota

in partial fulfillment of the requirements

for the degree of

Master of Science

Grand Forks, North Dakota

August

2014

This thesis, submitted by Damon Grabow in partial fulfillment of the requirements for the Degree of Master of Science from the University of North Dakota, has been read by the Faculty Advisory Committee under whom the work has been done and is hereby approved.

_____
Yeo Howe Lim, Ph.D.
Associate Professor Civil Engineering
Chairperson,

_____
Harvey Gullicks, Ph.D., P.E.,
Chair and Associate Professor Civil Engineering,

_____
Charles Moretti, Ph.D, P.E.,
Associate Professor Civil Engineering

This thesis is being submitted by the appointed advisory committee as having met all of the requirements of the School of Graduate Studies at the University of North Dakota and is hereby approved.

_____
Dr. Wayne Swisher
Dean, School of Graduate Studies

_____
Date

PERMISSION

Title   Satellite Derived Volumetric Soil Moisture in a HEC-HMS Model

Department   Civil Engineering

Degree   Master of Science

        In presenting this thesis in partial fulfillment of the requirements for a graduate
degree from the University of North Dakota, I agree that the library of this University
shall make it freely available for inspection. I further agree that permission for extensive
copying for scholarly purposes may be granted by the professor who supervised my
thesis work or, in their absence, by the chairperson of the department or the dean of the
School of Graduate Studies. It is understood that any copying or publication or other use
of this dissertation or part thereof for financial gain shall not be allowed without my
written permission. It is also understood that due recognition shall be given to me and to
the University of North Dakota in any scholarly use which may be made of any material
in my thesis.

                                    Name: Damon Grabow

                                    Date: August, 2014

TABLE OF CONTENTS

LIST OF FIGURES

LIST OF TABLES

ACKNOWLEDGMENTS

ABSTRACT

This research is intended to enhance recent hydrologic research that focused on a rainfall-runoff model of the Devils Lake basin in central North Dakota. This research employs the spatial volumetric soil moisture data collected by the National Aeronautics and Space Administration (NASA) Advanced Microwave Scanning Radiometer – Earth Observing System (AMSR-E) instrument. The AMSR-E data, collected from 2002-2011 from the NASA EOS Aqua satellite, was used in the Land Parameter Retrieval Model (LPRM) to estimate the surface soil moisture at a scale of 25-km. AMSR-E data is used in collaboration with the current rainfall-runoff model to better understand the influences of spatial soil moisture data on hydrology in the Devils Lake basin. The hypothesis is that the spatial volumetric soil moisture data will increase the accuracy of a hydrologic model based on single soil moisture data points.

The calibrated HEC-HMS model uses the soil moisture accounting method and produces a more accurate lake level hydrograph for Devils Lake. When comparing results from previous studies, this research produces an RMSE value of 0.85 ft during the same time frame in which previous studies produce values of 1.49 ft and 1.73 ft.

CHAPTER I

INTRODUCTION

1.1 Background

Soil moisture is an integral part of any hydrological system. It is the link between the

ground surface and atmospheric boundary layer within a water budget. "Soil moisture has been

identified throughout the new Decadal Survey, and may be the single most important parameter

linking the key components of hydrological, biological, and geochemical processes" (Owe, et al,

2008 and National Research Council, 2007). It has been shown that soil moisture can be a

driving factor in affecting precipitation events on the prairie landscapes (Raddatz, 2005). Even

though it has been demonstrated that soil moisture is a key to understanding complexities of our

environment, soil moisture data, historically, have not been widely attainable.

Soil moisture can often vary widely over a large spatial extent due to precipitation

patterns, terrain features, and both surface and sub-surface hydrology. However, the more

accurate data sets are in-situ single point measurements. While this type of measurement is good

for understanding localized phenomenon, it is not easily interpolated to a spatial data set. A

continental-scale or even global-scale data set would provide the best resolution for spatially

orientated soil moisture data. Developing a network of in-situ collection sites would prove to be

too costly. However, the space based remote sensing community has been developing and

enhancing satellite based soil moisture tools since the late 1970's (Owe, et al, 2008).

The first satellite based soil moisture sensing system was launched in 1978 aboard the

Nimbus-7 satellite and was decommissioned in 1987. The data collection system was the

Scanning Multichannel Microwave Radiometer (SMMR). The SMMR orbited Earth

approximately 14 times per day but required a total of 6 days to yield complete coverage of

Earth's surface.

Table 1. Soil moisture data collection satellites 1978 to 2008 (Owe, et al. 2008).

Parameter	SMMR	SSM/I	TMI	AMSR-E
Frequencies, GHz	6.6, 10.7, 18, 37	19.3, 36.5	10.7, 19.4, 37	6.9, 10.7, 18.7, 36.5
Polarization	H, V all frequation	H, V all all frequation	H, V all frequation	H, V all frequation
Incidence angle	50.2°	53.1°	52.88°	55°
Swath width, km	780	1394	759	1445
Orbit type	polar	polar	N38° to S38°	polar
Equator Crossing (Times in LST)				
Ascending orbit	1200 LST	1710 - 2131	Variable	1330
Descending orbit	2400 LST	0510 - 0931	Variable	130
Data period	1978 to 1987	Jul 1987 to pres.	Dec 1997 to pres.	May 2002 to pres.

The Special Sensor Microwave Imager (SSM/I) was launched in 1987 as part of the

Defense Meteorological Satellite Program (DMSP). The DMSP launched a total of 7 satellites

between 1987 and 2003, each carrying an SSM/I instrument. SSM/I had similar characteristics

to the SMMR except for the swath width being approximately 2 times of the SMMR and only

collected data at two frequencies, 19.3 and 36.5 GHz.

Tropical Rainfall Measuring Mission (TRMM) Microwave Imager (TMI) was underway

in 1997. The focus of TMI is on the tropics, as its orbit falls between the 38° North and 38°

South latitudes. TRMM is based on SSM/I technology and collects data at similar frequencies but also includes 10.7 GHz. Due to the tropical orbit it circles the earth 16 times per day.

The data used for this research were collected by the Advanced Microwave Scanning Radiometer (AMSR-E) platform onboard the AQUA Earth observation satellite that was launched in 2002. However similar to SMMR, AMSR-E orbits Earth daily and had nearly total coverage between the 45° North and 45° South and roughly 80% beyond those latitudes.

1.2 Soil Moisture Data for Hydrologic Modeling

A water budget describes water movement and storage within a watershed. Input components of a water budget include precipitation, groundwater discharge, riverine inflow, and overland inflow while output components include evaporation and evapotranspiration, riverine outflow, groundwater recharge. Also included in the water budget equation are areas of storage. Storage within a water budget includes surface storage and subsurface storage. One variable that makes up subsurface storage in the water budget is soil moisture. Soil moisture, or volumetric water content, can be defined as water stored in the pores within the soil. The quantity of soil moisture can determine the types of flora and fauna within a local ecosystem and determine the capacity of the soil to absorb moisture, significantly affecting the hydrologic response to precipitation events (van der Valk, 2005). Direct point measurement of soil moisture is more accurate, however, it has limitations due to the lack of spatial coverage and cost. However, there are few observational soil moisture data sets available for research. The Natural Resources Conservation Service (NRCS) operates the Soil Climate Analysis Network (SCAN, www.wcc.nrcs.usda.gov/scan/) across the country but only maintains two soil moisture stations near the Devils Lake basin; site #2020 in Mandan, ND and site #2050 at the Glacial Ridge research center near Mentor, MN. In the case of Devils Lake, both of these sites are more than

100 miles away, taking away from the contributing value to Devils Lake research. However, based on averaged monthly soil moisture values from the National Weather Service Climate Prediction Center (www.cpc.ncep.noaa.gov) and average annual precipitation data from the National Weather Service (www.weather.gov) it could be argued that the Mandan, ND site is viable to represent conditions in Devils Lake, ND. These data show that Mandan, ND and Devils Lake, ND fall within the 200-300 mm zone while the Mentor site falls within the 300-400 mm zone. The average annual precipitation varies from Devils Lake, ND by 6.6 in (Mentor, MN) and 2.6 in (Mandan, ND). Another data collection system is the AmeriFlux site and Data Exploration System operated by the Oak Ridge National Lab. Like the SCAN data sites, the AmeriFlux sites are sparsely populated over the US. The nearest sites to the Devils Lake basin are in Brookings, SD and Minneapolis, MN. The AmeriFlux volumetric soil moisture data at Brookings are comprised of two depths, one meter and two meter (http://ameriflux.ornl.gov). The National Weather Service Climate Prediction Center estimates spatial soil moisture of the continental US, but the data are not suited for research due to generalized moisture contours. A common way to take account for soil state is the use of the Curve Number system, as shown by Melesse, et al. (2006) in a study that estimated the surface water balance for the Devils Lake basin. Typically, the Curve Number method is used as a gridded dataset.

There are numerous hydrologic and climatologic models focused on Devils Lake. However, many of these models concentrate on one discipline, such as the atmospheric boundary layer, surface water hydrology, and stochastic hydrology (Vecchia, 2008). Models that incorporate a multitude of these disciplines are computationally prohibitive or are lacking in some area. The lack of scientific aggregation leads to a disconnect between the sciences. For example, in the natural world, surface water interacts with soil, ground water, and the

atmospheric boundary layer. However, it is uncommon to see one model incorporate in-depth tools that use all fields. There are a number of ways to retrieve soil moisture data. Minet et al. (2011) demonstrated the usefulness of ground penetrating radar in collecting soil moisture data. Ground penetrating radar yields data on a field scale, allowing for multiple points in a small area. However, the radar data produce an investigative depth of 5-10 cm.

Recent missions by the National Aeronautics and Space Administration (NASA) have collected data with potential to allow for connectivity between surface water and sub-surface water in a modeling environment. NASA's Advanced Microwave Scanning Radiometer – Earth Observing System (AMSR-E) instrument, collected from 2002-2011 from the NASA EOS Aqua satellite, was used in the Land Parameter Retrieval Model (LPRM) to estimate the spatial volumetric soil moisture at a scale of 0.25 degree resolution. "LRPM is a three-parameter retrieval model for passive microwave data and is based on a microwave radiative transfer model that links surface geophysical variables (i.e., soil moisture, vegetation water content, and soil/canopy temperature) to the observed brightness temperatures" (Teng, et al. 2010). The LPRM data have been validated in past research to provide reliable data collection platform. "LPRM soil moisture has been extensively validated over a large variety of landscapes, using in situ, models, and other satellite soil moisture products, and has an accuracy of about 0.06 $m^3\,m^{-3}$ for sparse to moderate vegetated regions" (Teng, et al. 2010). Wang et al. (2009) found agreement with the AMSR-E data and local soil moisture probes in northern China.

1.3 Objectives of Research

It is the objective of this research to compare a hydrologic model utilizing spatial soil moisture data to one that does not utilize observed source soil moisture data. Hydrologic modeling efforts at the University of North Dakota have produced a calibrated rainfall-runoff

model of the Devils Lake basin using the initial and constant soil moisture method in the Army Corps of Engineers HEC-HMS. The Master's thesis by Hassell (Hassell, 2010) discusses the development of a rainfall-runoff HEC-HMS model. Elaboration on the Hassell model (Munna 2012 and Lim et al. 2012) was done by incorporating a reservoir model, HEC-ResSim, along with Global Circulation Model data that estimate precipitation and temperature out to 2050. This research will employ the spatial volumetric soil moisture data collected by the NASA AMSR-E in collaboration with the current rainfall-runoff model to better understand the influences of spatial soil moisture data on hydrology in the Devils Lake basin. Satellite derived soil moisture data have been shown to be effective at increasing the accuracy of rainfall-runoff models. In one example of this approach, Brocca el al. (2010) used the soil wetness index from the Advanced SCATterometer (ASCAT) that was onboard the Metop satellite from the Netherlands Institute for Space Research to produce a more accurate hydrologic model. It is expected that the spatial volumetric soil moisture data will increase the accuracy of a hydrologic rainfall-runoff model and also highlight sensitivities of spatial soil moisture variation on surface runoff.

1.4 Study Area

The Devils Lake basin, located in north central North Dakota and in the Prairie Pothole region of the Upper Great Plains, has been the focus of scientific research nearing the past century. Devils Lake is a closed basin system in the northern Great Plains that covers approximately 3810 square miles (North Dakota State Water Commission, 2010). Although the basin is said to be a closed system, a natural outlet does exist but not below the elevation of 1458 feet above mean sea level (amsl) which has been surpassed three times in the last 4000 years as depicted in Figure 1. A closer look at more current levels is shown in Figure 2, below.
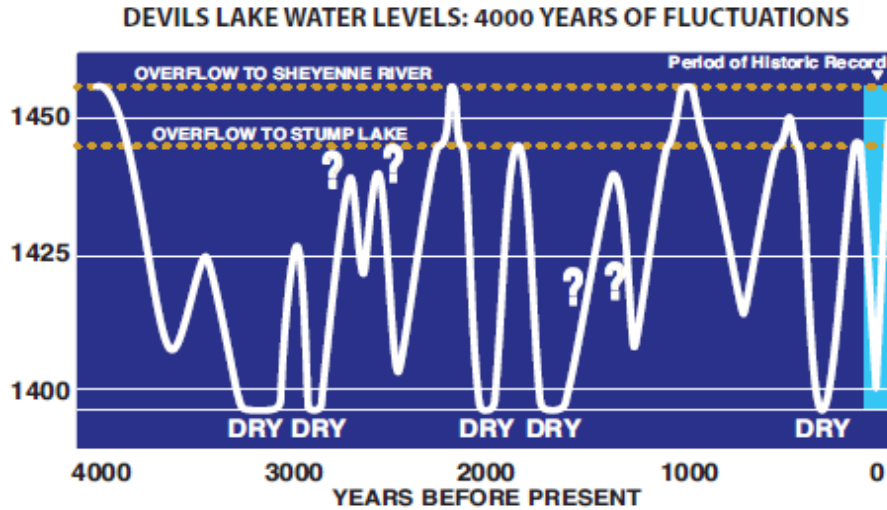
Figure 1. Historic lake elevations of Devils Lake (NDSWC, 2010).
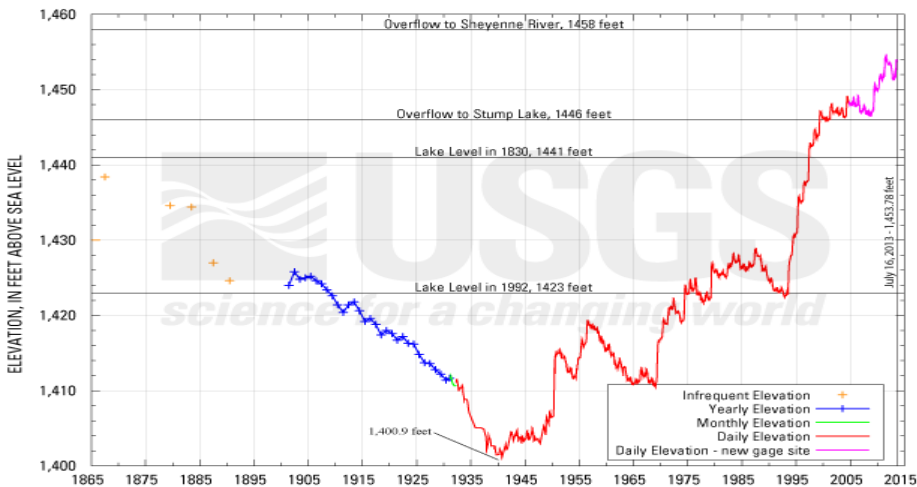
Figure 2. USGS recorded lake levels for Devils Lake up to 2013
(http://nd.water.usgs.gov/devilslake/data/dlelevation.html)

This region is made up of mostly grasslands and a dense population of wetlands that are closely linked to climatic wet-dry cycles that can range from 5-35 years (van der Valk, 2005). The region was also affected by the last glacial ice age, which left the underlying soils as glacial till made up of clay and silt (Gerla and Matheny, 1996). This type of soil combination does not allow for a high rate of sub-surface water movement, which in turn leads to the susceptibility of ponding. Generally, the Prairie Pothole region has little terrain relief and thus few large river

systems. Thus, the Devils Lake basin carries all of these traits and is sensitive to climate shifts. Given the lack of relief in the region the watersheds are difficult to discern, and in many cases are split depending on slight rises in water levels.

The basin is subject to continental effects of weather and climate. These changes in local weather and regional climate cause the lake levels to rise and fall in dramatic fashion, the historic low in 1940 was 1402 feet above sea level while most recent high was in 2011 at 1454.3 feet amsl as shown in Figure 1 below (U.S. Geological Survey, N.D). The current rise in lake levels, not only in Devils Lake proper but basin wide, has had a significant impact on the region. Combined, money spent on research and fighting lake levels by the state, federal, and local agencies total to more than $1 billion (U.S. Army Corps of Engineers, 2010). These projects addressed road and railroad elevations, dikes and levees, property buyouts, drainages, futuristic climate models, lake level frequency analysis, pumping stations, and building razing, etc.

CHAPTER II

MODEL HISTORY AND METHODOLOGY

2.1 Model History

The hydrologic models preceding this study were the foundation to the development of a

research platform. Each model iteration adds to the depth and sophistication throughout the

development process. Hassel (2010) constructed the hydrology model of Devils Lake using the

United States Army Corp of Engineers' HEC-HMS model. This work led to the study completed

by Munna (2012) which used NASA precipitation data (TRMM) to supplement calibration data

for HEC-HMS modeling and also introduced Global Climate Model (GCM) downscaled climate

data. The GCM data, in conjunction with the improvements to the HEC model produced by

Hassel, was then used to forecast futuristic hydrologic fluctuations to the year 2050.

The purpose for this study is to focus on determining the feasibility of NASA's LPRM

soil moisture data. The simulation is based off of the model produced by Munna (2012).

However, there are changes to the modeling approach in order to accommodate the soil moisture

data. Munna (2012) used the initial and constant loss method, while this model uses the soil

moisture and accounting method (SMA). The purpose of using the SMA method is to build a

model that is better suited to continuous simulation that is based on natural conditions. Hassel

(2010) and Munna (2012) completed the hydrologic model. Therefore, the background work

needed for model development has also been finished. Terrain analysis for the delineation of

watersheds, with the use of ArcGIS and ArcHydro, along with

EXPLANATION
— · · — · · — BASIN BOUNDARY
— · — · — · — SUBBASIN BOUNDARY
▲ DEVILS LAKE GAGE

1. Mauvais Coulee (879.13, 20)
2. Calio Coulee (234.96, 9)
3. Edmore Coulee (519.47, 15)
4. Starkweather Coulee (273.81, 16)
5. Little Coulee + Comstock Coulee (506.15, 13)
6. Stump Lake (348.72, 22)
7. Devils Lake North (445.33, 1)
8. Devils Lake South (350.42, 1)
9. Devils lake (206.46, 1)

Major subbasins in the Devils Lake Basin.
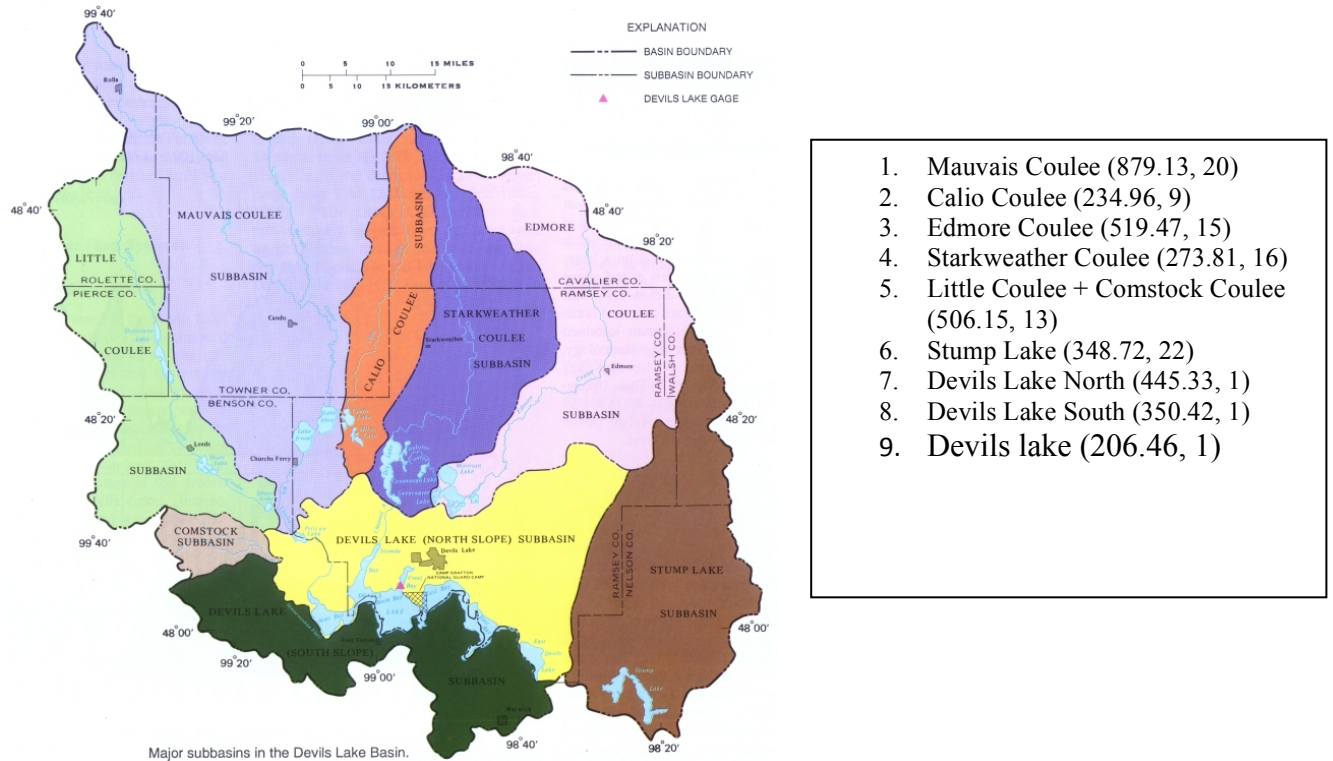
Figure 3. Map of the Devils Lake sub-basins (USGS, N.D) with sq. mi. and # sub-areas.

hydrologic calculations and calibrations through the use of HEC-HMS and HEC-ResSim have all

been completed. The original hydrologic parameters in HEC-HMS included the initial and

constant loss method and the SCS unit hydrograph transform method. HEC-HMS describes the

'initial and constant' method in two phases. First, the initial loss determines precipitation that is

infiltrated or stored prior to surface runoff occurring. Second, the 'constant' loss describes the

rate of infiltration once the 'initial' parameter is met. The Initial and Constant loss method is

found to be suitable for single event based modeling versus long term continuous modeling.

However, with the inclusion of the LPRM data the model will need to be adjusted to use the

SMA loss method. SMA allows for model interpretation of water movement throughout the soil

column using 18 separate parameters. These parameters account for water movement both into

and out of the soil column by estimating the amount of water capture and movement through 5

separate layers. The 2 upper most layers are the vegetative canopy and surface storage, which both require an estimated percent full and initialization and a total storage (in). The soil layer also requires an estimated percent full at initialization and total storage (in), but also requires the maximum infiltration (in/hr), tension storage (in), and soil percolation (in/hr). The percent of impervious land area is required. The groundwater consists of two layers, upper and lower aquifers, and includes storage capacity (in), percent full at initialization, percolation rate (in/hr), and a coefficient that describes the lag time to achieve baseflow. The SCS unit hydrograph transform method will continue to be utilized.

2.2 Model Inclusion of LPRM

The LPRM data retrieved from NASA dates from 2002-2006 for this project. These dates coincide with the calibrated Munna (2012) model. LPRM data were on a 25-km grid with an upper left corner at 48.875 North latitude and 99.875 West longitude and a lower right corner at 47.875 North latitude and 98.375 West longitude, as shown in Figure 4.
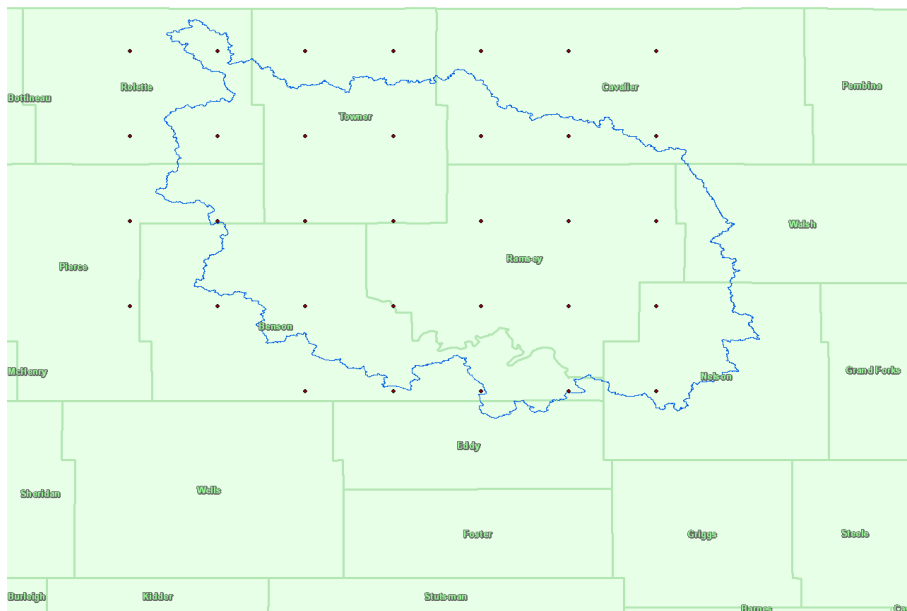
Figure 4. LPRM data points shown throughout the Devils Lake basin in NE North Dakota.

NASA provided a website for data retrieval,

http://hydro1.sci.gsfc.nasa.gov/opendap/hyrax/ncml/LPRM_AMSRE_D_SOILM3_timeSeries.ncml.html.

Examples of the website and data format are provided in Appendix C. Not all of the available

soil moisture data covers North Dakota, so the data from NASA is limited to a night-time

satellite pass (LPRM_AMSRE_D_SOILM3). The data comes as a time series at a single point,

so the users is required to have previously obtained the study area bounding box and the number

of data points needed. The site asks for longitudinal and latitudinal steps from the origin at -

179.875, 89.875 in longitude/latitude coordinates. Each step is 0.25 degrees; there are 1440

longitude steps and 720 latitude steps.

HEC-HMS called for each individual subbasin to need its own soil moisture parameter.

This allowed for any basin wide spatial variation to be accounted for within the data set up.

Because of this, the nearest LPRM point was noted for each subbasin centroid.

HEC-HMS called for the soil moisture percentages to fulfill the initial condition portion

of the model set up. The initial condition was utilized by the model to build a baseline starting

point, after which the model estimated the soil moisture. LPRM data was volumetric soil

moisture percentage and was plugged into the model straight away without alteration.

2.3 Loss Model

The loss method selected for this project was the SMA loss method. SMA allows the

user to enter antecedent soil moisture values at the initiation of the model window. This

approach uses multiple layers that incorporate water movement throughout the local system both

above ground and below.

Above ground variables in SMA include both canopy and surface moisture storage percentages and percentage of impervious surfaces. This allows for land use variation within a sub-basin or throughout a watershed. Canopy and surface required values include both the percentage of storage filled and the total amount that the system is capable of storing. The canopy storage value represents precipitation captured by the vegetation that is never allowed to reach the ground. Also, canopy storage can only be removed by evaporation. The surface storage value represents water captured in small depressions on the surface. Surface storage can move into the soil as infiltration or into the atmosphere as evaporation.
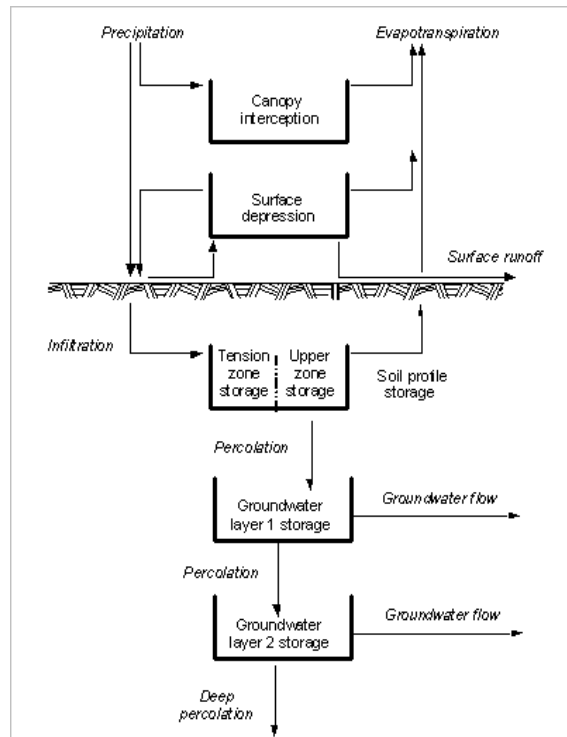
Figure 5. Schematic of USACE HEC-HMS soil moisture accounting loss method. (USACE Tech Manual, 2000).

Below ground variables in SMA include max infiltration rate, 3 versions of groundwater, soil storage, tension storage, and soil percolation. SMA uses the maximum infiltration rate set by the user as the upper limit of a linear function between infiltration from the surface to the soil.

SMA divides groundwater into three segments. 'Soil' is the top section of soil at the surface and is defined by the user with units in percentage of storage filled and in inches. Water can pass into soil storage as infiltration and be removed as evapotranspiration or percolation. The rest of the groundwater portion is broken into to 'groundwater' sections that divide the groundwater movement into shallow and deep portions. Again, these are set by the user with percentage stored and total possible stored. The groundwater parameters can be omitted in order to simplify areas of storage given soil types and local phenomenon.

Infiltration is water available to enter the soil column from the surface component. HEC-HMS estimates the volume of water available for infiltration using Equation 1, below.

$$Potential\ Soil\ Infil. = Max\ Soil\ Infil. - \frac{Current\ Soil\ Storage}{Max\ Soil\ Storage}\ Max\ Soil\ Infil. \qquad (1)$$

In the case of this study, the saturated conductivity values (KSAT), found within the Natural Resource Conservation Service's (NRCS) Soil Survey Geographic database (SSURGO), and were used in the model as the maximum soil infiltration parameter. SSURGO KSAT values are described as "the amount of water that would move vertically through a unit area of saturated soil in unit time under unit hydraulic gradient" within the NRCS SSURGO Metadata Table Column Description report (http://www.nrcs.usda.gov/wps/portal/nrcs/detail/soils/survey/?cid=nrcs142p2_053631). These data were averaged spatially to estimate a single value per subbasin. The mean average was calculated over the three zones in the vertical soil column within the SSURGO data and the units were changed from (μm s^{-1}) to in hr^{-1} to satisfy HEC-HMS data requirements (in/hr). This process was done using ArcGIS' Spatial Analyst Zonal Statistics. Shown below is a graphic of the KSAT values per subbasin over the study area.

Percolation is the transfer of water from the soil layer to the groundwater or aquifer layers. The user defines the maximum value for the percolation parameter. The percolation at each time step is defined in Equation 2, below. In the case where the groundwater layers are omitted for simplicity, the percolation out of the soil layer is still allowed but the groundwater storage layers can be dropped from the equation. Also, as the volume of water available to the percolation equation gets reduced the percolation rate also is reduced due to the reduction in the Current Soil Storage value.

$$Potential\ Soil\ \mathrm{Perc.} = Max\ Soil\ Perc.\left(\frac{Current\ Soil\ Storage}{Max\ Soil\ Storage}\right)\left(1 - \frac{Current\ Groundwater\ Storage}{Max\ Groundwater\ Storage}\right) \qquad (2)$$

Legend

ksat_avg_dl
aveKSAT_us
| 1.0295 - 1.0848 |
| 1.0849 - 1.1762 |
| 1.1763 - 1.2614 |
| 1.2615 - 1.4022 |
| 1.4023 - 1.5959 |
| 1.5960 - 1.7949 |
| 1.7950 - 2.3079 |
| 2.3080 - 3.0814 |
| 3.0815 - 5.3142 |
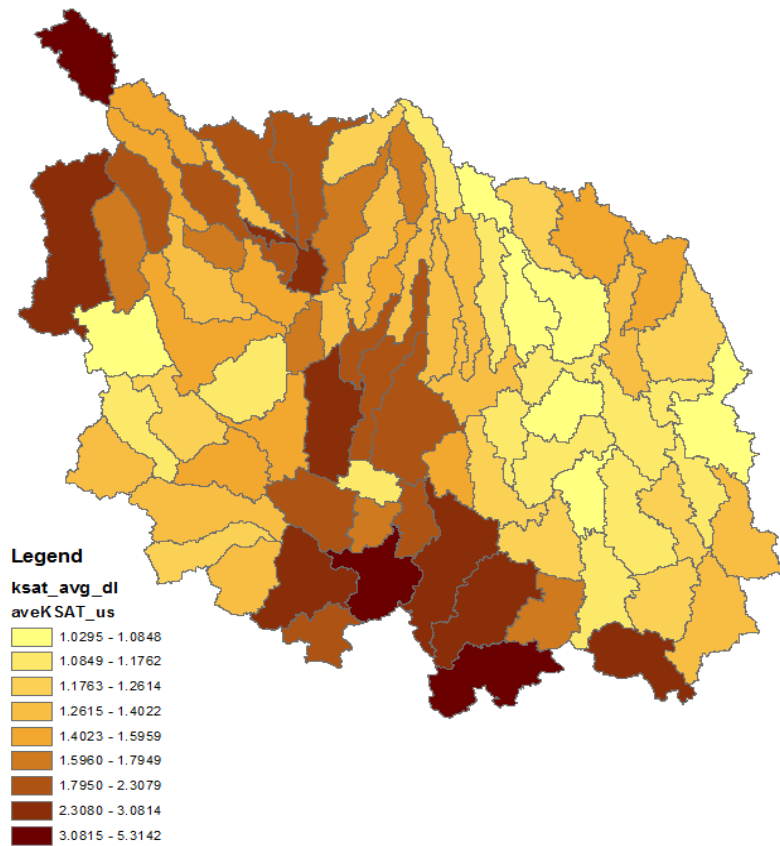
Figure 6. SSURGO KSAT values (in/hr) averaged over each sub-area.

The evapotranspiration parameter represents the transfer of water from the surface, canopy, and soil layers to the atmosphere. HEC-HMS calls for the user to submit an evaporation table that is used to estimate evapotranspiration values. The model estimates the amount of moisture needed to satisfy the evapotranspiration total then removes that moisture from, first, the canopy storage, then surface storage, and finally the soil layer. If these layers were not enough to satisfy the ET value and moisture is removed from the tension layer. Equation 3, below, represents ET in the model. The function of Current Soil Storage and Max Tension Storage is a two criteria approach. The first criteria is that (Current Soil Storage/Max Tension Storage > 1) water is available to be transferred to the atmosphere at a 1:1 rate. However, if criteria 1 is not met, criteria 2 is utilized, in which the ET decreases as time increases using Figure 7, below.

$$Acutal\ Evaporation\ Soil\ =\ Potential\ Evaporation\ Soil\ \cdot\ f(Current\ Soil\ Stor., Max\ Tension\ Stor.) \quad (3)$$
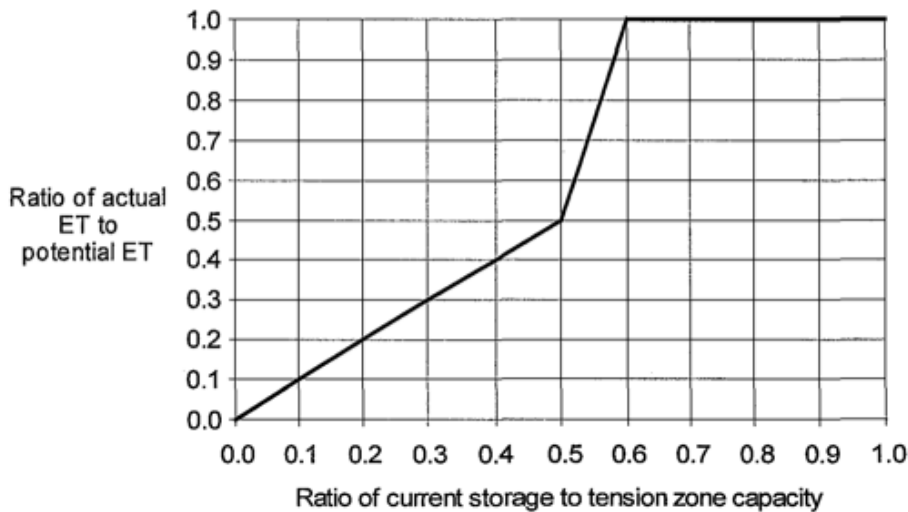
Figure 7. ET as a function of tension storage (Bennett, 1998).

The combination of equations and set of criteria are utilized within HEC-HMS in a specific order. The criteria are based on the occurrences of precipitation or ET. ET is not

estimated during any time step where precipitation occurs. Precipitation is used to fill the 'buckets' of the layers in Figure 5 from the top down, the canopy to the groundwater layers. Once the layers are filled equations 1, 2, and 3 are used to transfer the water over time. If there is no precipitation during the time step, ET is estimated. In similar order to that of the precipitation allotments, ET is first estimated using the canopy and continues downward until the potential ET volume is met.

2.4 Climate Data Inputs

The primary driver for any hydrologic model is the meteorological dataset. These data include precipitation, temperature, and evaporation for the HEC model. In many cases there are numerous collection stations and data types for weather data. This study uses data downloaded from the North Dakota Agricultural Weather Network (NDAWN) and the National Weather Service. Continuous temperature and precipitation data were gathered from the NDAWN Langdon, ND and Cando, ND station data (July 1998 to December 2013), also found in Appendix B. Evaporation data were found in the National Weather Service Technical Report 34 (Farnsworth and Thompson, 1982).

The precipitation data include rain and snow amounts, recorded in inches of water equivalent. This allows for continuous modeling over the winter months and into the spring snowmelt season. The need for year-round modeling is due to the significance of the spring runoff, as spring is the period of highest peak discharges into Devils Lake.

Evaporation data are taken as a monthly average. Data from the Devils Lake, ND site (Farnsworth and Thompson, 1982) are averaged for every month. However, this data assumed no evaporation during winter months; November – March. This was found to be valid when

compared to current evapotranspiration data collected at the Cando NDAWN site and by

Vecchia (2008).

Table 2. Monthly averaged PET values from TR-34 and NDAWN site at Cando.

	Jan	Feb	Mar	Apr	May	Jun	Jul	Aug	Sep	Oct	Nov	Dec
TR-34 @ DL	0	0	0	3.57	6.08	6	6.94	6.17	3.96	3	0	0
NDAWN Cando	0.0197	0.0288	0.0561	0.149	0.218	0.2352	0.2306	0.2077	0.1631	0.0896	0.0379	0.0187

CHAPTER III

MODEL SENSITIVTY

3.1 HEC-HMS Model Discussion and Sensitivity

The USACE HEC-HMS model is a common hydrologic model to use when studying

surface water hydrology. HMS has a robust toolkit that allows users to incorporate just about

any data set into a model. Not only does HMS work as a stand-alone hydrologic model, it

accepts data from other platforms that includes GIS data, USGS gauge data, radar precipitation

data, or custom databases with the use of USACE's DSSvue software. DSSvue acts as the go

between from outside sources and also as a model output viewer for HMS. This combination of

software is used worldwide and locally; University of North Dakota, North Dakota State Water

Commission, UNESCO in Sudan, and Jadavpur University of Kolkata, India are four examples.

HMS, being as widely used as it is, efficiently performs the task for which it is designed.

Specifically, the SMA loss method performs well. The SMA method does allow for the

integration of a wide degree of data sets like soil moisture and soil conductivity. This study

found the soil moisture data to be most useful in short term model runs of 1-3 months, although

the model was shown to be capable of longer model runs of 1+ years.

However, the SMA loss method does have its deficiencies. Even though the method has

the capabilities to accept 18 different variables of the each of the sub-basins, many of them fall

short of their importance to model completion. The canopy and surface variables are

questionable in their effect on model outcomes and have even been removed from the model all

together in version 3.5. The overall effect of the soil moisture variable, even though it has a

multitude of effects on the local environment, is on model outcomes minimized due to the

inclusion only at model initialization.

When comparing the sensitivity of the soil moisture data on model outcomes it was found

that similar results were observed for any soil moisture data, even when the sample soils were set

to saturation levels of 100% soil moisture. Shown below is a graph depicting the sensitivity of

the soil moisture data when initializing the SMA loss method model. Per Figure 8 below, there

is no change in outflow estimation while the soil % input is changed. Even if the initialization

data is a bit off, it is shown to correct to the observed data over time during a long model run as

shown in Roy et al (2013). This study used observed soil moisture data for the initialization

period; however, the model would be more robust if allowed to use a time-series soil moisture

data set.
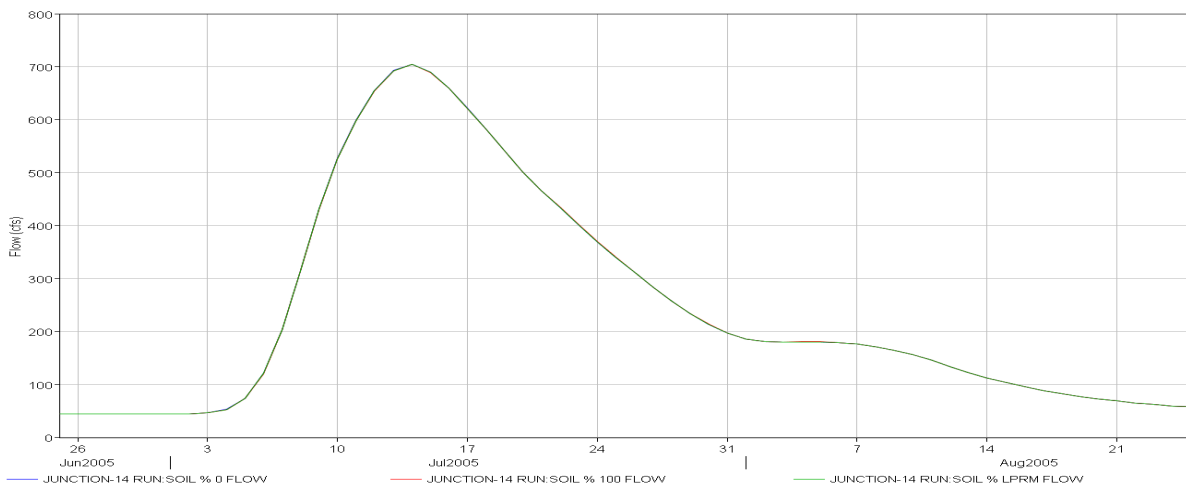
Figure 8. Comparison of outflow from models with differing soil % inputs (NASA LPRM, 0%, and 100%).

Canopy storage capacity and percent full are two variables that are required for the SMA loss method. As stated above, the initialization values for these variables were 0.2 in and 20%, respectively, in the Mauvais Coulee model. Model sensitivity to these variables was explored by comparing the above values to extremes. In the case of the canopy storage, 0.2 in was compared to 0 in and 0.5 in. In the case of the canopy percent full, 20% was compared to 0% and 100%. These data are displayed in Figures 9 and 10. The difference in canopy percent full amounted to 6.4%. Peak values at 0%, 20%, and 100% were 708.2 cfs, 704.4 cfs, and 753.1 cfs, respectively. The difference in canopy storage peaks was 11.5%. Peak values at 0 in, 0.2 in, and 0.5 in were 726.9 cfs, 706.5 cfs, and 798.6 cfs, respectively. The intuitive trend for the canopy is that the lower initialization percentage would create more storage in the canopy layer at the model start. Also, that the lower canopy storage capacity would in turn yield higher run off values. However, that trend is not held up in this case. The middle value for both variables produces the lowest peak cfs, counter to the expected trend stated earlier.
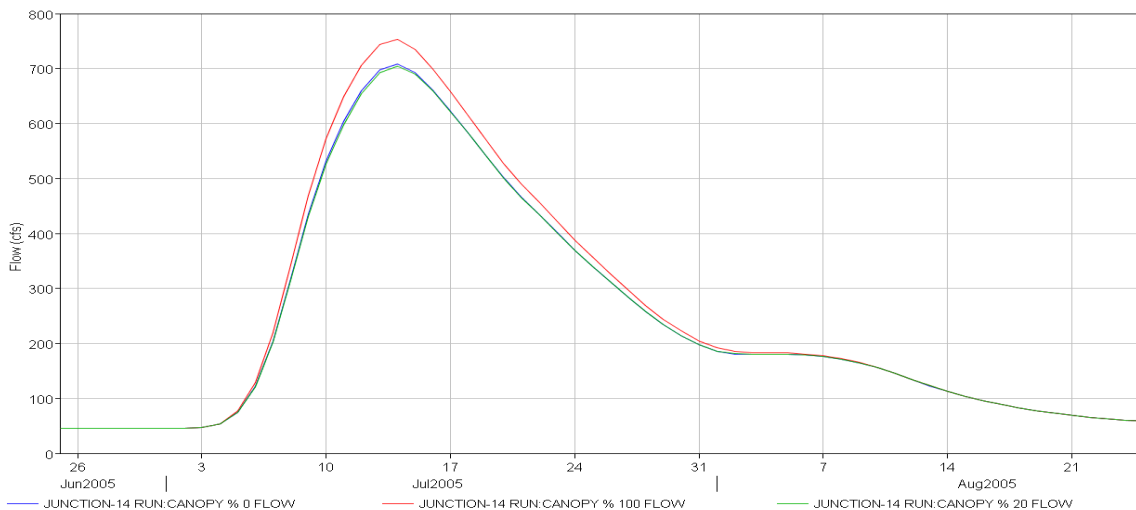
Figure 9. Sensitivity of canopy percent full using 0%, 20%, and 100%.
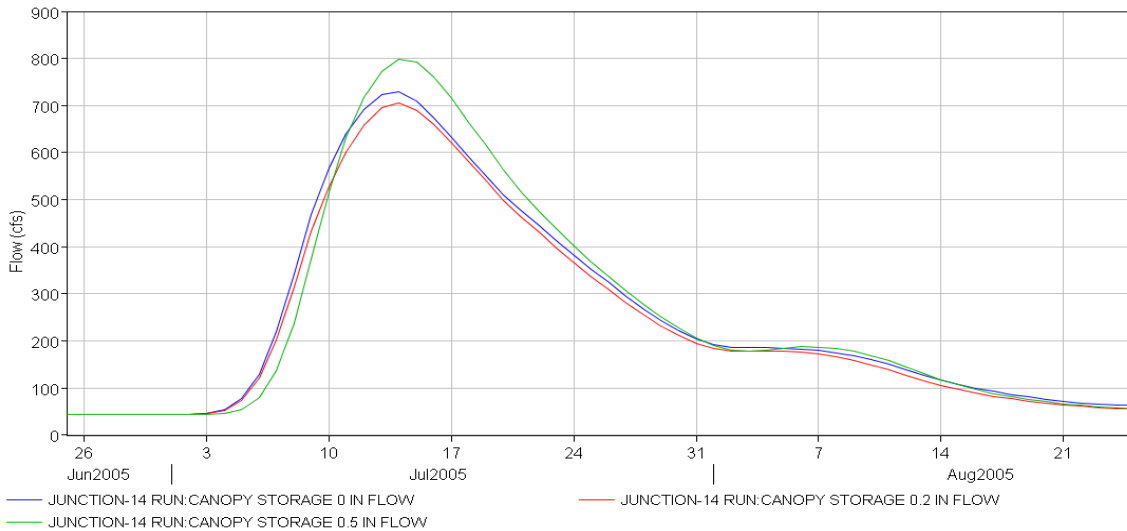
Figure 10. Sensitivity of canopy storage using 0 in, 0.2 in, and 0.5 in.

Another pair of variables that were looked at during the sensitivity analysis was the surface storage and percent full. These variables represent the water content within the surface of the soil layer. Just like the approach of the canopy variables, the initialization values were compared to extreme values both low and high. The surface percent full initial value was set to 20% and compared to 0% and 100%. The surface storage initial value was 0.2 in and compared to 0 in and 0.5 in. Depictions of comparable hydrographs are shown below in Figures 11 and 12. Surface percent full peak outflow values were found to 702 cfs, 706 cfs, and 704.4 cfs, respectively at 0, 20, and 100 percent. Surface storage capacity peak outflow values were found to be 879 cfs, 633 cfs, and 552.9 cfs, respectively at 0, 0.2, and 0.5 inches. With regards to surface percent full, any percent full at initialization produced similar peak flow values. The surface storage variable was found to more sensitive with a difference of 37% from the extreme peak outflows. This is due to the models' usage of soil storage capacity in infiltrating the water versus only producing runoff.

22
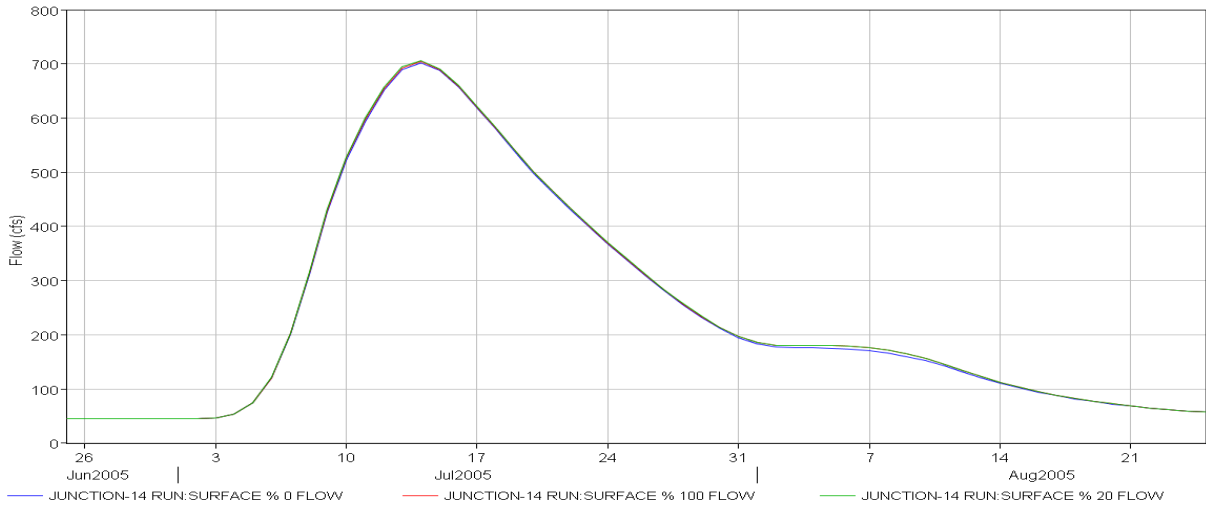
Figure 11. Comparison of surface storage sensitivity analysis (0%, 20%, and 100%)
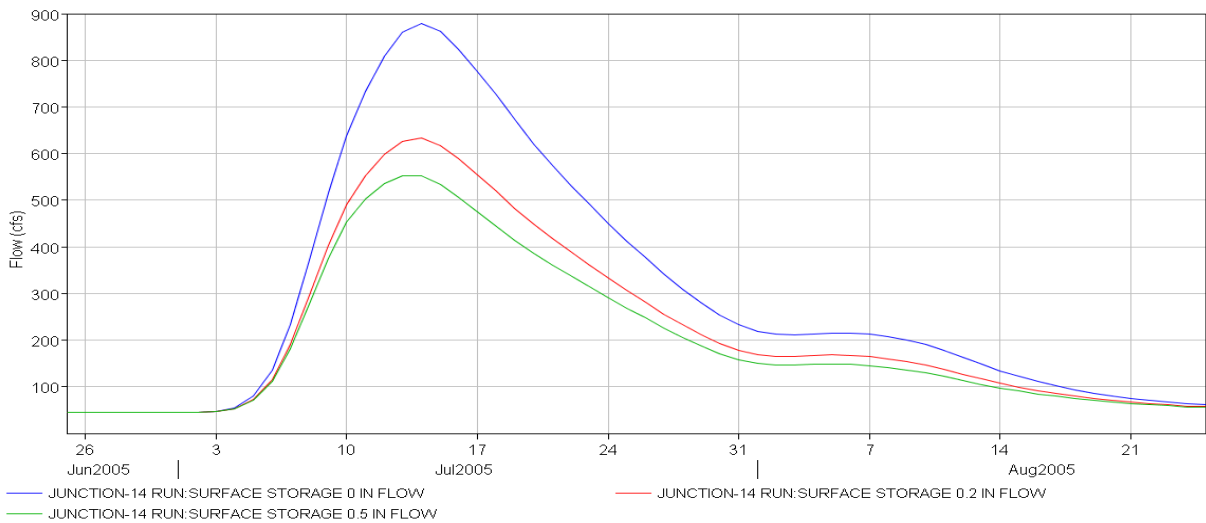
Figure 12. Comparison of surface storage sensitivity analysis (0 in, 0.2 in, and 0.5 in)

Another variable from the sensitivity analysis was tension storage. Tension storage is the water retained within the soil column due to friction. Typically, this value is small and the initial value used within the model was 0.05 in. During the sensitivity analysis the initial value was compared to 0 in and 0.1 in and the peak outflow was the indicator of sensitivity. Peak outflow values were 528.4 cfs, 704.4 cfs, and 2428.3 cfs for the 0 in, 0.05 in, and 0.1 in model runs

respectively resulting in a 78% difference. Depictions of the tension storage values are shown below in Figure 13.
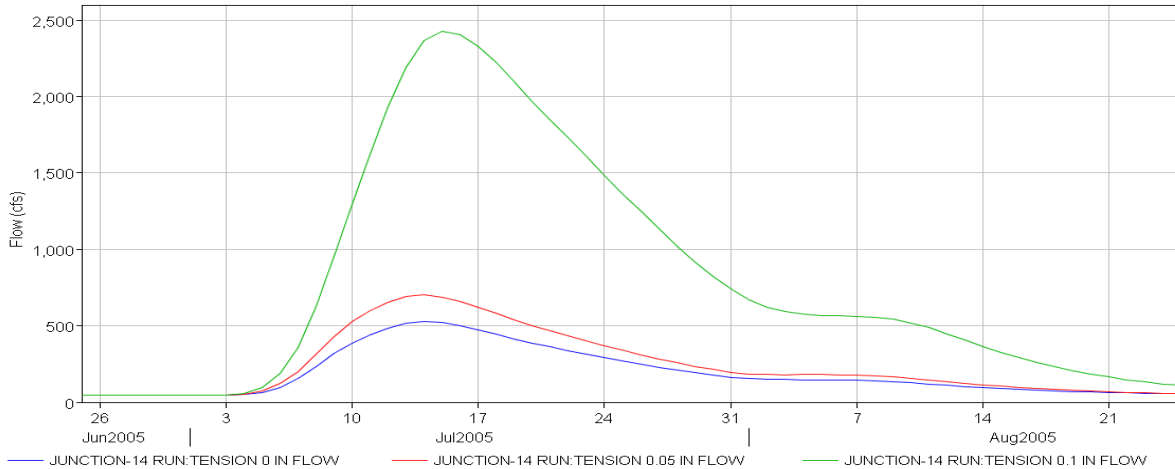
Figure 13. Comparison of soil tension sensitivity model runs (0 in, 0.05 in, and 0.1 in)

The last variable within the sensitivity analysis was soil percolation. The soil percolation parameter represents the movement of water in the soil column from the tension zone to the groundwater zone. Even though the groundwater was not used within this model the soil percolation parameter had an influence on model sensitivity. Soil percolation had a strong influence on not only the event used for calibration but the sensitivity of the following event as well. Low values of soil percolation produced a rebound affect to the hydrograph that oscillated up and down getting closer to zero flow the farther it got from the event. The comparison hydrographs are shown below in Figure 14. Values used for the sensitivity analysis were 0 in/hr, 0.03 in/hr, and 0.1 in/hr. Model sensitivity to the soil percolation parameter was demonstrated during the event. An unusual post-event peak rebound effect was noted. Peak values for the analysis were 2429.4 in/hr, 704.4 in/hr, and 470.8 in/hr, respectively for 0, 0..03, and 0.1 percolation rates.
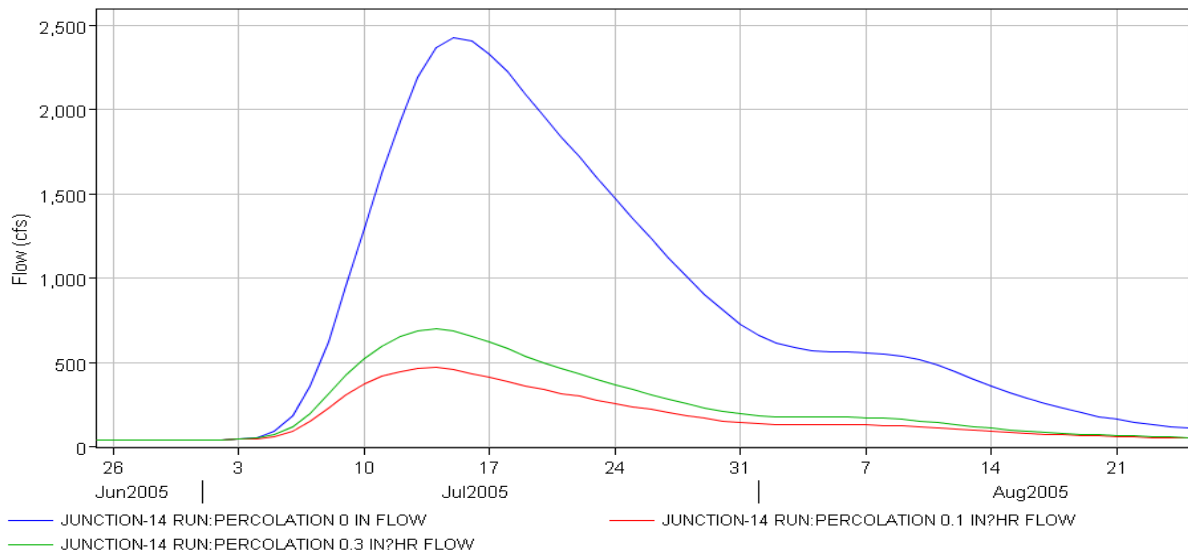
Figure 14. Soil percolation sensitivity analysis outputs (0 in/hr, 0.03 in/hr, and 0.1 in/hr)

CHAPTER IV

MODEL CALIBRATION

4.1 Calibration Approach

Model calibration was completed in two steps; adjusting the environmental variables for

comparison against observed stream gauge data in the Mauvais Coulee sub-basin and adjusting

the variables against the observed levels of Devils Lake. In both cases, samples of short term

events were calibrated first followed by a large scale calibration event covering multiple years.

The focus of the Mauvais Coulee calibration was on loss parameters while the snow melt

parameters and evaporation were the drivers for the lake elevation calibration. Also, sensitivity

analyses were conducted to check their effects on model outputs.

4.2 Stream Calibration

First, the model was calibrated based on local stream flow observations from USGS

station 05056100 along the Mauvais Coulee near Cando, ND (shown in Figure 15). Along with

the observed data, the long term calibration run from Munna (2012) was used as a comparison

for acceptance. Calibrations were focused on the Mauvais Coulee sub-basin within the Devils

Lake basin. The Mauvais Coulee is located in the northwest corner of the Devils Lake basin

(Figure 2), and is also the largest sub-basin.

The dates chosen for the summer rainfall event calibration were July 1 – August 31,

2005. These dates were chosen based on the flow levels. This period had a low level event with

a peak near 737 cfs with an event length of approximately one month. Once the model

calibration was complete, three other events were used as verification events. These events were

recorded in June of 2002, September of 2002, and a long term model run from 2002 - 2005. The

verification events yielded similar outflows to that of the calibration event, were of similar

duration, and were found to be strictly rainfall events.
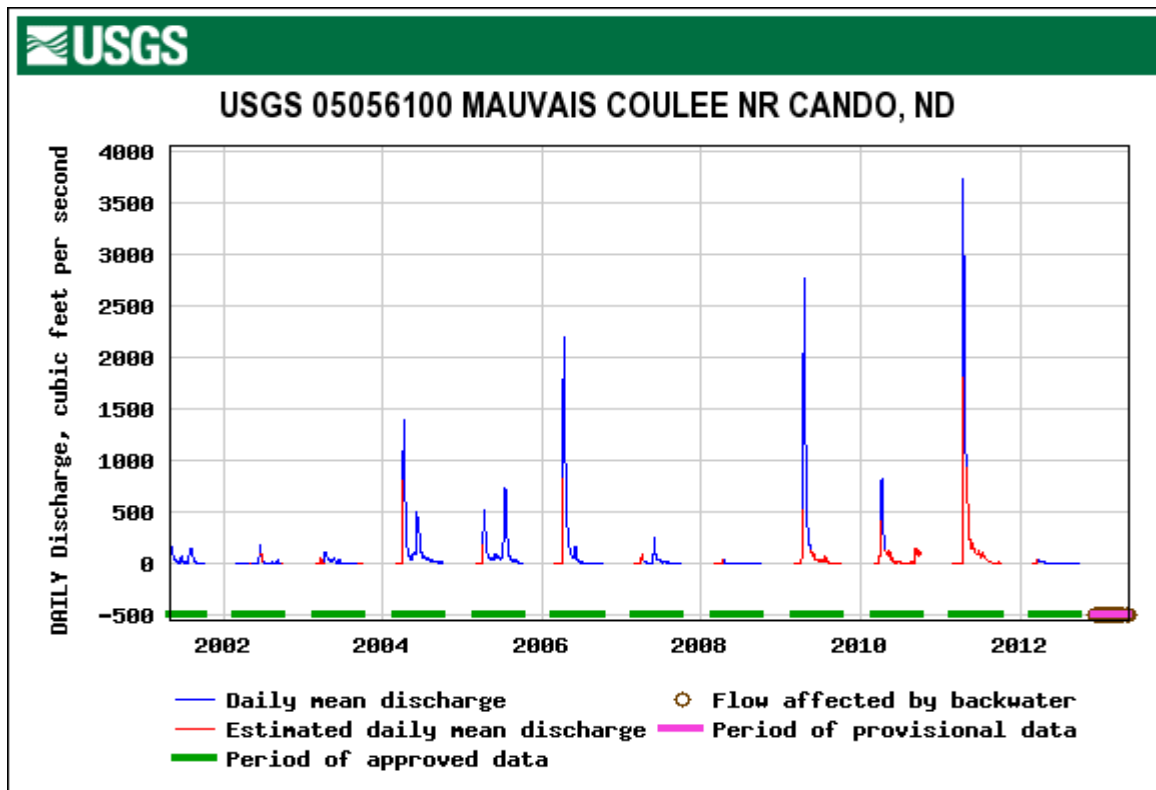
Figure 15. USGS data collected at the Cando observation site.

The SMA loss method calls for a wide variety of parameters, 18 in total, which include

data for the canopy down to a second groundwater layer and much in between. Table 3, below

goes through all of the variables and the values used for this study. The parameters work

together to construct a model that is intended to mimic nature.

The parameters in the upper most portions of the hydrologic column are the canopy and surface parameters. These two make up the storage capacity of the local environment at or above the surface of the ground and include storage within the vegetation and on the surface of the ground. For this study, the canopy and surface percent full parameters were assigned starting values of 20% and 100%, respectively, and 2 maximum storage capacities of 0.2 inches.

Impervious surface % was also required. The study region consisted of rural areas, and thus, was found to have an impervious surface % between 0-10%. Therefore, for this study the impervious surface % used was 4% based on GIS data.

Table 3. Example of model values for the observed data at Mauvais Coulee.

Subbasin	Canopy %	Surface %	Soil %	GW 1 %	GW2 %	Canopy St.	Surface St.	Max Infil.	Imp. %	Soil St.	Tension St.	Soil Perc.
4	20	100	20	0	0	0.2	0.2	0.798411	4	0.2	0.15	0.05
3	20	100	20	0	0	0.2	0.2	0.9630935	4	0.2	0.15	0.05
2	20	100	20	0	0	0.2	0.2	0.879686	4	0.2	0.15	0.05
7	20	100	20	0	0	0.2	0.2	0.829762	4	0.2	0.15	0.05
17	20	100	20	0	0	0.2	0.2	0.646877	4	0.2	0.15	0.05
1	20	100	20	0	0	0.2	0.2	1.3038715	4	0.2	0.15	0.05
12	20	100	20	0	0	0.2	0.2	0.865448	4	0.2	0.15	0.05
6	20	100	20	0	0	0.2	0.2	0.8260235	4	0.2	0.15	0.05
5	20	100	20	0	0	0.2	0.2	1.0376175	4	0.2	0.15	0.05
10	20	100	20	0	0	0.2	0.2	0.947649	4	0.2	0.15	0.05
9	20	100	20	0	0	0.2	0.2	1.1152255	4	0.2	0.15	0.05
13	20	100	20	0	0	0.2	0.2	0.687872	4	0.2	0.15	0.05
8	20	100	20	0	0	0.2	0.2	0.815598	4	0.2	0.15	0.05
18	20	100	20	0	0	0.2	0.2	1.22016	4	0.2	0.15	0.05
11	20	100	20	0	0	0.2	0.2	1.127142	4	0.2	0.15	0.05
20	20	100	20	0	0	0.2	0.2	0.829762	4	0.2	0.15	0.05
14	20	100	20	0	0	0.2	0.2	0.718783	4	0.2	0.15	0.05
15	20	100	20	0	0	0.2	0.2	0.7235245	4	0.2	0.15	0.05
16	20	100	20	0	0	0.2	0.2	0.857755	4	0.2	0.15	0.05
19	20	100	20	0	0	0.2	0.2	0.879686	4	0.2	0.15	0.05

The upper tier of the soil column was associated with a number of model parameters. Just like the canopy and surface, the upper tier of the soil column also called for an initial %, which is the % of total available soil moisture. NASA's LPRM soil moisture data was inserted

into the model here. This data represents natural conditions for the initialization of the model; inputs are displayed in Table 3 above. Along with the soil moisture %, the upper tier of the soil column calls for total amount of storage. This parameter is the total amount of water that the soil is capable of storing before further infiltration into the groundwater parameters. During the calibration of the model, it was found that the best fit value for soil storage was 0.2 inches. The last parameter needed to complete the upper tier of the soil column was the maximum infiltration value. This value is the highest rate of soil conductivity on average per subbasin. Values used for this study were the KSAT (saturated conductivity) values taken from the Natural Resources Conservation Service (NRCS) SSURGO (Soil Survey Geographic Database) data set. The estimated values gathered from the subbasin averaging were generally between 1.5 and 2.5 in/hr. However, it was found during the calibration that these values were best suited when divided by 2, such that the calibration values were generally between 0.75 and 1.25 in/hr.

Tension storage, or the water held in the upper bounds of the soil column that is not removed by gravity, was found to be best represented with 0.15 inches. In addition to tension storage, soil percolation was also assigned a value for this study. The soil percolation value was uniform over the study area and 0.05 in/hour was found to best represent the region.

Groundwater portions of the model were omitted. The region is predominantly made up of glacial till which inhibits surface water discharge to underground aquifers (van der Camp and Hayashi, 1998). Vecchia (2002) and Wiche (1994) have shown that ground water influences in the region specific to Devils Lake have little to no effect on the lake during wet cycles.

Obs Flow vs. NASA LPRM Model Flow
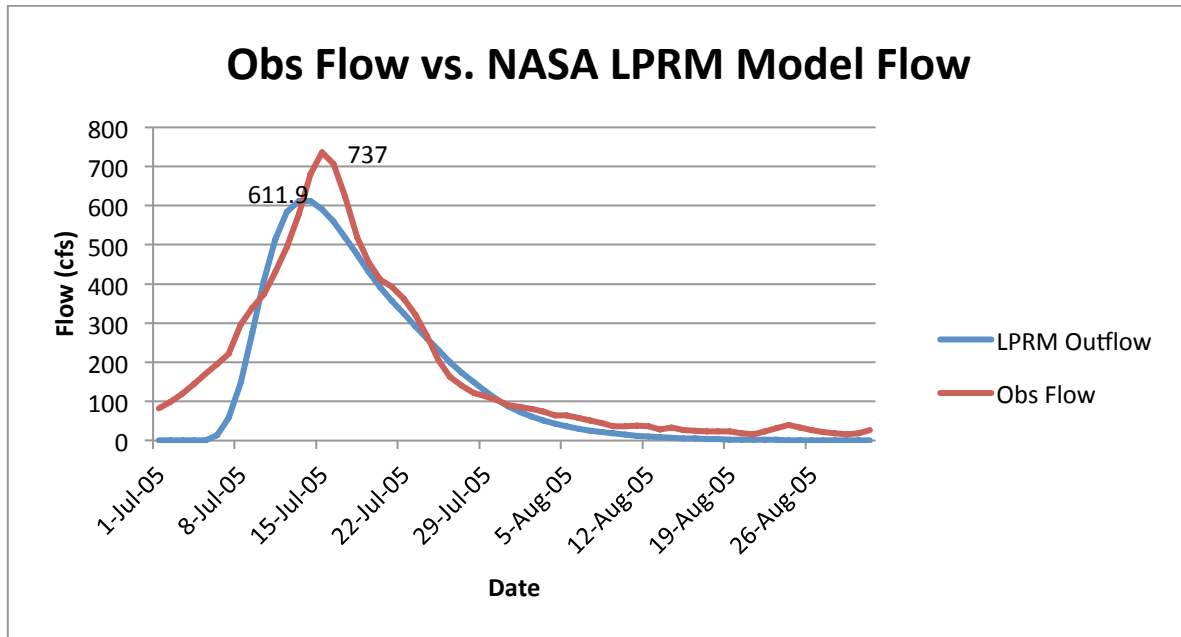
Figure 16. Hydrographs from the observed data and NASA LPRM model output for the calibration run.

The model calibration run was conducted over July 1, 2005 to August 15, 2005. Observed flows from this event, at Junction 14 within the HMS model, peaked at 737 cfs on July 15, 2005. Overall, the model calibration was done by trial and error to find the parameters that best fit the observed data curve. The focus of the calibration was to closely match the observed flows. The observed flow curve had three characteristics that were relied upon during the calibration; the timing of the peak flow, the height of the peak flow, and the shape of the curve. Shape of the hydrograph is subjective; however, the focus of the shape is on the leading and tailing slopes of the hydrograph. Shape was adjusted using the SMA parameters, lag times, and routing times. The timing of the peak flow was done by manipulating the sub-area lag times, or the time of the center of rainfall to the peak of the hydrograph for each sub-area. The height of the peak and the curve of the hydrograph were manipulated using the SMA loss parameters. Shown in Figure 16 are hydrographs of the calibration model run comparing the observed data

and the model output. The model performed well, with a peak value of 611.9 two days prior than the observed data.

Verification June 2002

Verification September 2002
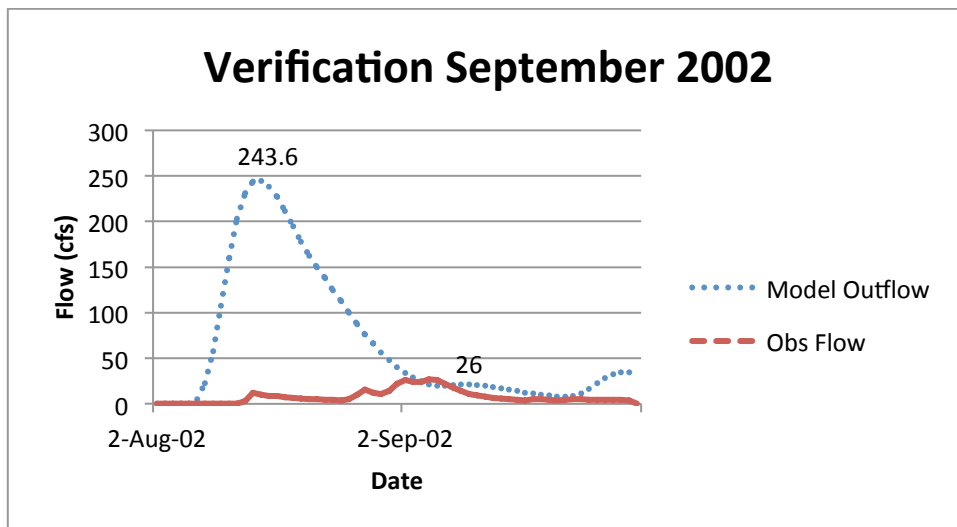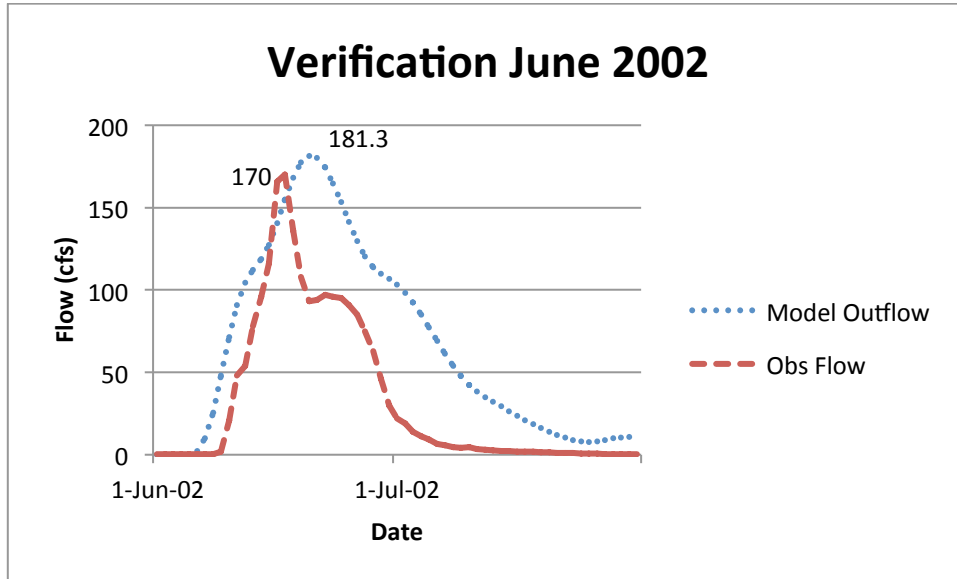
Figure 17. Hydrographs of the verification flows versus observed flows, June 2002 and September 2002.

Although the calibrated storm performed well when compared against the observed data, there were varying results during the verification of the model. The calibrated model was verified using two short-term events similar to the calibration event and again using a period of 4

years for a look at the long term capabilities of the model. The two short term events were June 2002 and September of 2002, while the long term model ran from 2002 – 2005. However, only one verification event performed well. The June 2002 and September 2002 verification events produced r-squared values of 0.62 and 0.0192 respectively. Shown below are hydrographs depicting the comparison between the modeled verification events and the observed data.
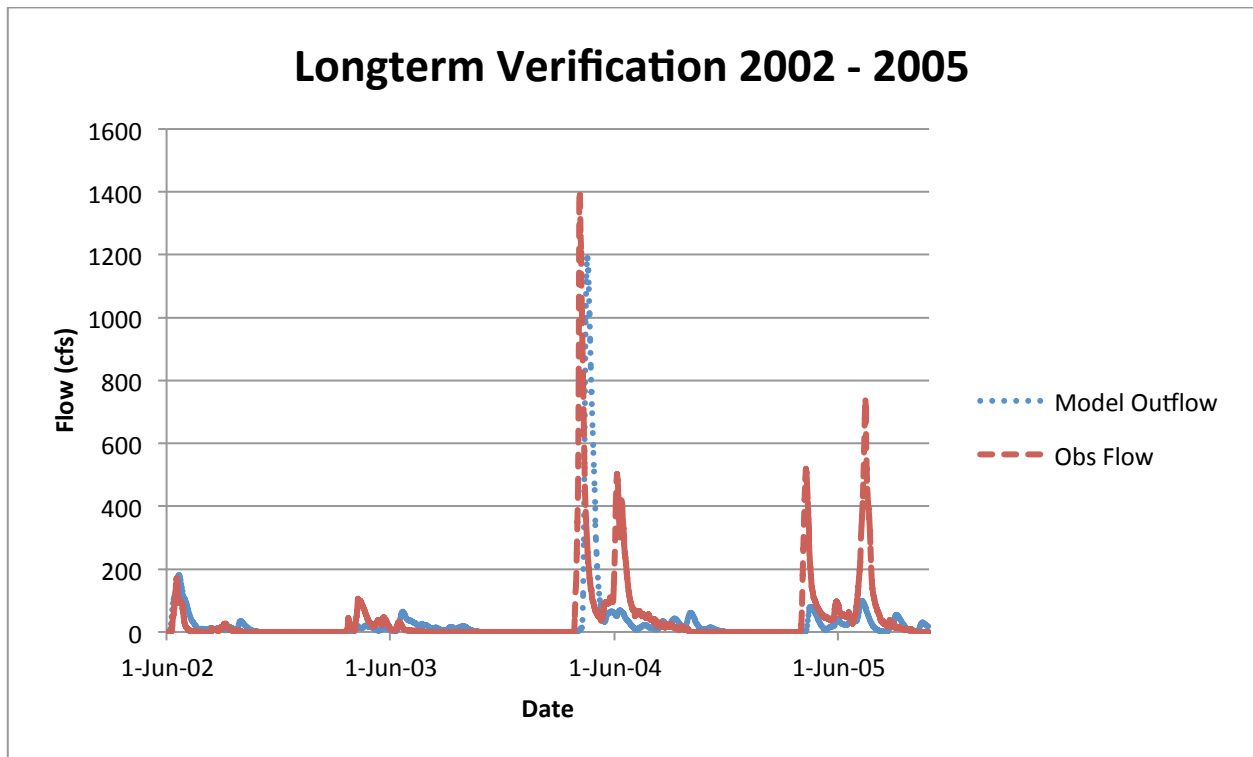
 Figure 18. Long term model run, June 2002 to October 2005 at Mauvais Coulee, Junction-14 in HEC-HMS model.

The SMA loss method in HEC-HMS was designed to run over long term periods by accounting for water loss throughout the soil column. It has been shown that this approach is capable of producing a respectable result when compared to observed data, Roy et al. 2013. The final step in the calibration process for this study was to verify the model over a longer period than the calibration event. The study area was located in a region that is normally frozen during the winter months and Munna (2012) has accounted for precipitation type, snow melt, and

temperature change at or near freezing. Thus, it was expected that the model would perform fairly well going into the transition from winter to spring by accounting for the snow melt timing and amount. The verification run started with the calibration storm, June 2002, and ran for just over one year to the end of October 2005. The focus of this model run was the timing and runoff volume values during the spring snow melt.

When comparing the long term NASA LPRM model run to the observed data from 2002 – 2005 (Figure 18) there are a number of similarities and differences. First, the peaks of the data are a good fit; 1189.6 cfs for the model and 1390 cfs for the observed come out to a 15% difference. Also of note is the June 2002 event at the start of the run. As discussed above, the model fits the observed data fairly well. Second, the tendencies of the model in representing the smaller flow events are poor. The observed peaks less than 800 cfs are severely under estimated in the model. Thus, leading to a significant under estimation of the total outflow volume; 73941.9 ac-ft for the model compared to 111197.06 ac-ft for the observed data. In the end, it appears that the model represents the observed data poorly.
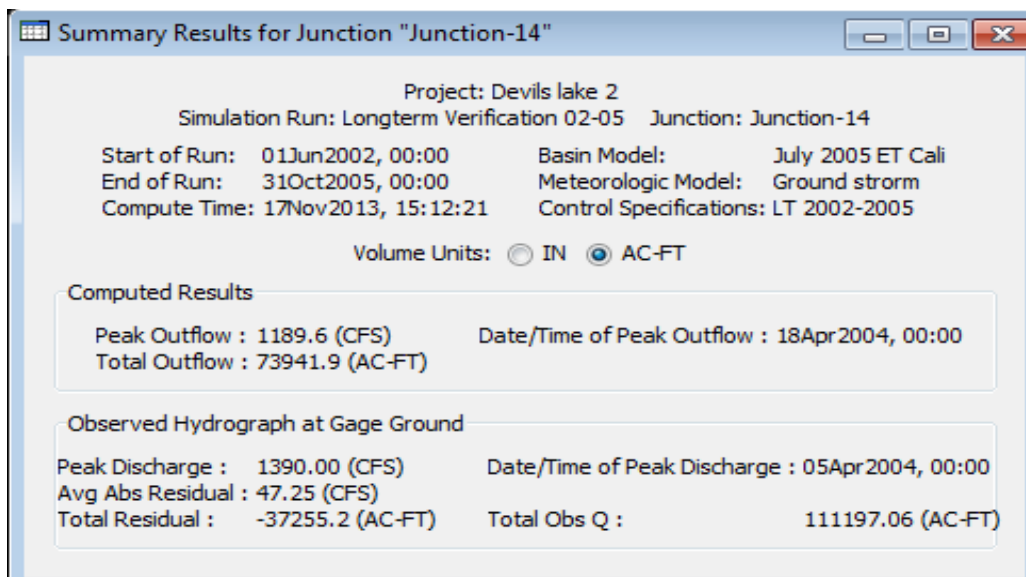
Figure 19. HEC-HMS statistical output comparing the long term model to observed data.
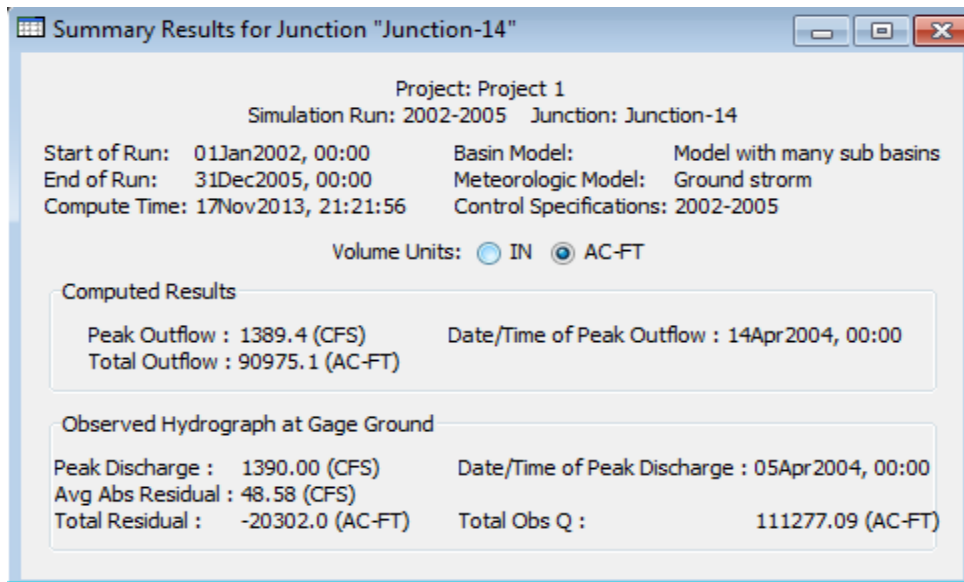
Figure 20. HEC-HMS statistical output comparing the long term model from Munna (2012) to observed data.

In the same comparison of the Munna (2012) model and the observed data it was found that the Munna (2012) model represents the observed data a bit better. Statistics in Figure 20 above show that the both the peak and total outflow volume better represent observed data. The peak discharges during the modeled period were 1390 and 1389.4 cfs for the observed and Munna (2012) model, respectively. In the same regard, the total outflow volume was represented by the Munna (2012) model as 90975.1 ac-ft compared to the observed 111277.09 ac-ft (a 18.3% difference).

4.3 Lake Calibration

Secondly, and the focus of this study, the model was calibrated based on the gauge recordings at Devils Lake along the Creel Bay (USGS site 05056500, "Devils Lake NR Devils Lake, ND). These data were recorded at two sites along Creel Bay (south Creel Bay from 1930 – 2004 and North Creel Bay from 2004 – present day). Although, two sites were used the data

were continuous with no shifts in datum. Shown above is a hydrograph of the Creel Bay

recording stations on Devils Lake (Figure 21).
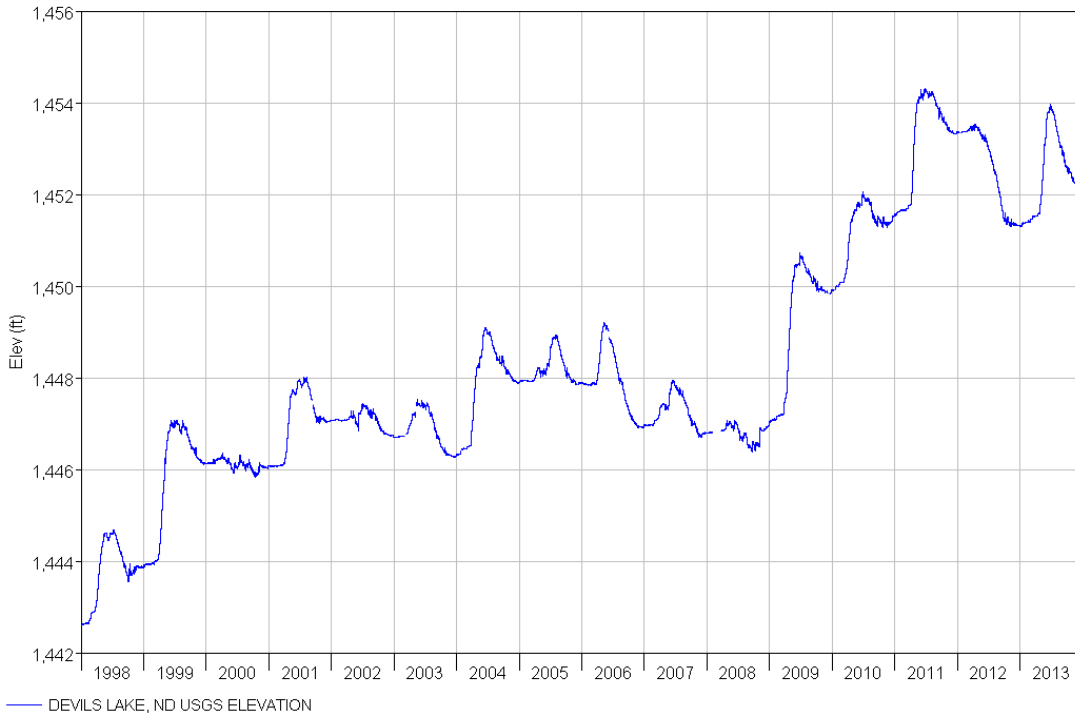
Figure 21. Lake elevation data from Creel Bay on Devils Lake (1998-2013)

Like the stream calibration, the lake calibration consisted of 3 shorter time windows

followed by a long duration system calibration. During the calibration the lake levels were the

only output parameter considered. The calibration focus was the late spring and early summer

months due to the fact that the majority of lake inflows come from springtime snow melt runoff.

Calibration for the lake elevations was broken into three sections; 1998 – 2003, 2004 – 2009,

and 2010 – 2013. It was found during the calibration that these three breakpoints represented

differing hydrologic regimes over the entire study time period. The first section ran from 1998 –

2003, and the data trend had a moderate upward data slope of 0.0016 resulting in an actual

elevation change of 3.71 ft, as shown in the plot below in Figure 22. The second section ran from

2004 – 2009 and had a downward slope of 0.0008. Even though the trend during this time was

downward, the lake levels rose from 1446.29 (2004) to 1447.05 (2009), resulting in an actual

+0.76 ft rise. Lastly, the section from 2010 – 2013 had the greatest change in actual lake levels:

+5.23 ft with an average data slope of 0.0022.
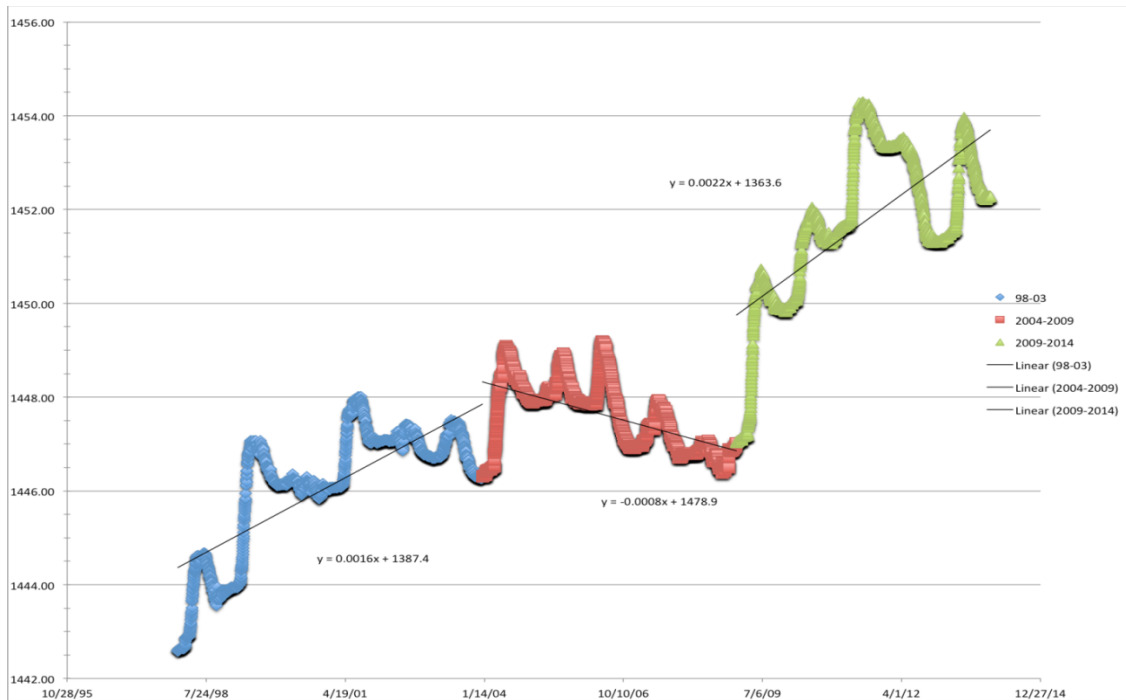
Figure 22. Devils Lake hydrologic regimes plotted with trend lines.

      Since the calibration of the lake levels was focused mainly on the spring runoff, the

parameters used in the calibration were different than those for the stream calibration. HEC-

HMS has a series of parameters that define snowmelt. These parameters consider boundary

layer air temperatures, snowmelt rates with and without rain, and snowpack water holding

capacity. The base temperature and PX temperature describe the freezing point and the point of

changing precipitation type and are set to 32° F and 33.5° F respectively. The melt rate and wet

melt rate describe the normal melting rate versus the melt rate during a rain event; for this study

they were set to 0.01 IN/DAY and 0.24 IN/DEG F-DAY, respectively. The cold limit and ATI-

Coldrate Coefficient describe the temperature within the snowpack and were set to the

recommended values of 0.8 IN/DAY and 0.84, respectively. The water capacity, set to 0.1%,

describes the water in the snowpack available for runoff. The groundmelt is the amount of snow

melted by heating from the ground, it is set to 0 IN/DAY here. Lastly, the ATI-meltrate function

is a user defined function that defines the meltrate curve for a particular area. The function used

in this study is shown in Table 4, below.

Table 4. ATI Meltrate function used to estimate snowmelt in HEC-HMS.

ATI (DEG F -DAY)	Meltrate (IN/DEG F-DAY)
-36	0
-20	0
0	0
32	0.1
34	1
36	1.5
38	2
40	2.75
42	3.5
44	4.25
46	5
48	5.75
50	6.5
52	7.25
54	7.35
56	7.45
58	7.55
60	7.65
62	7.75
64	7.85
66	8
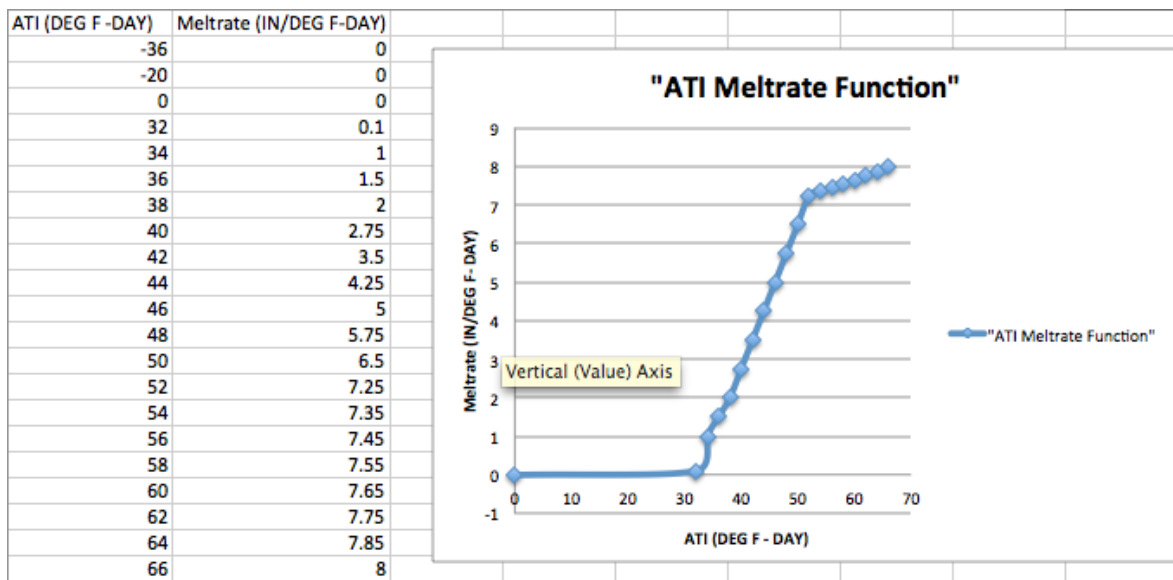
Due to the section breaks within the study period many of the parameters were adjusted

to find the best fit for each calibration run. And it was found that for short time periods, 3-5

years, the model was able to perform well. However, outside of the small window of success the

natural environment fluctuates too widely to be predicted by a single formula. This is evident by

the three time periods chosen here. The first, 1998 – 2003, shows moderately increasing lake

levels while the second, 2004-2009, shows moderately decreasing lake levels, and the third, 2010

– 2013, shows more dramatic lake inflows. This all occurs during a period in which precipitation

does vary with winter precipitation snow water equivalent 3.233 IN, 3.36 IN, and 4.84 IN in the

first, second, and third time periods, respectively. Interestingly, 2004 -2009 had a higher average

winter precipitation than 1998 – 2003 but yielded a negative effect on lake levels. Another note

is that the late summer/fall precipitation of 2010 – 2013 is more than double of the other two

sections, meaning the soil was holding more water heading into the winter months.
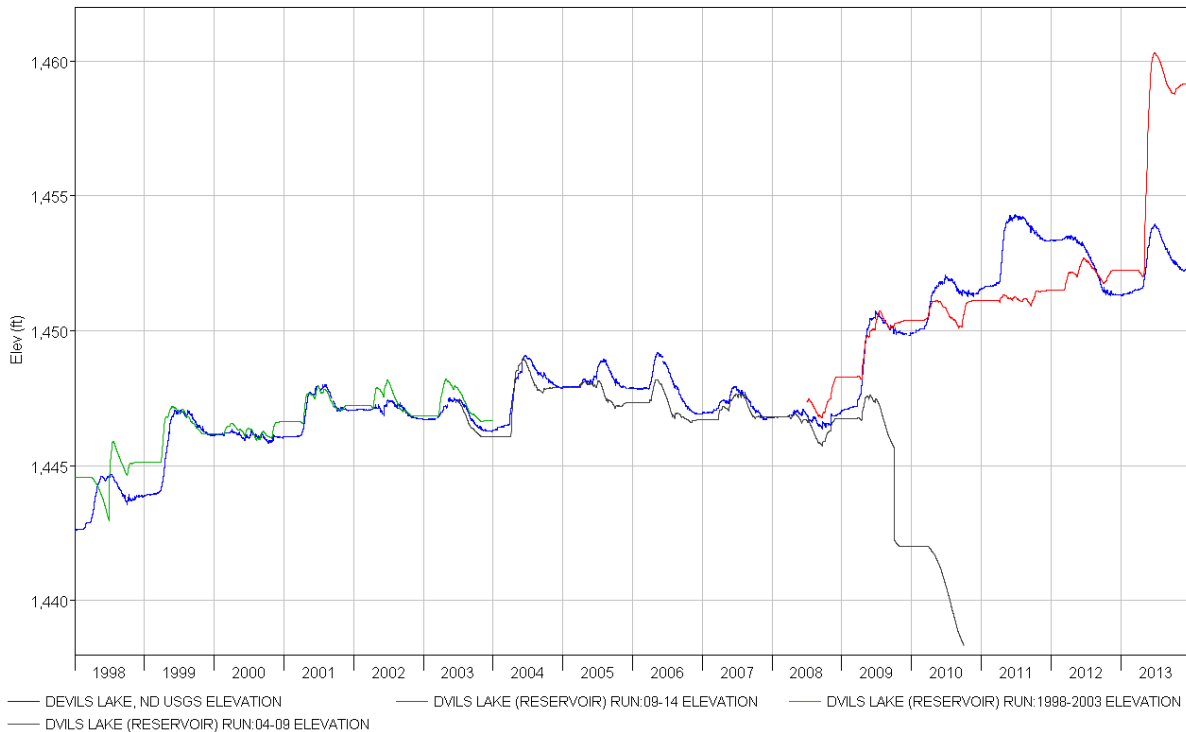
Figure 23. Hydrographs comparing model outputs to recorded lake levels.

Table 5. Comparison of peak timing and peak discharge for each model run.

Model Run	Ave Diff Peak Day	Ave Diff Peak CFS
98-03	6.33	-0.6855
04-09	13.6	0.548
09-13	22	-0.6

Each of these three short models were then run independently for the entire length of the

study, 1998 – 2013. The outputs were compared to find the best fit model parameters for a long

term or continuous model. Parameters were unchanged for the initial comparison, but the

hydrograph best representing the observed data was then adjusted for a better fit.

The hydrograph produced from the 2004-2009 data was the worst fit of the three.

Because of the model was built to fit the negative trend in the observed data it does a poor job

during times of positive lake levels. However, the timing of the spring runoff events was good

and the peaks of those events compares well to the other two model runs.
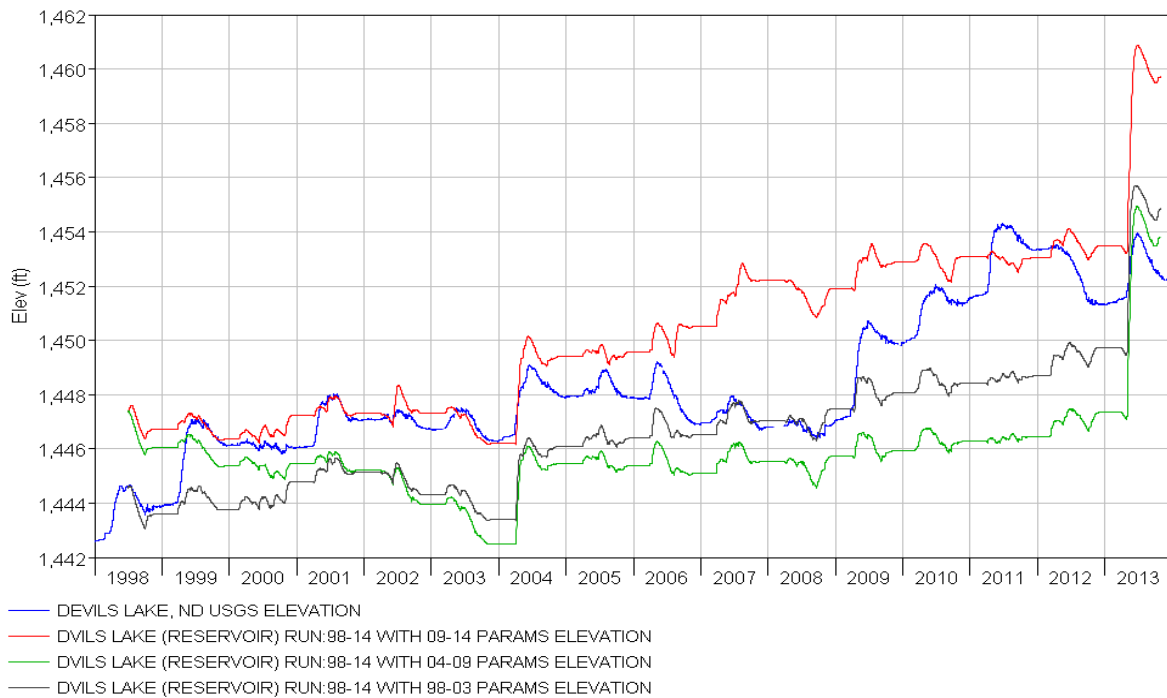
Figure 24. Hydrographs comparing long term outputs.

Hydrograph results from the 1998 – 2003 model run were slightly better than the 2004-

2009 model. The model was built with a slope of +0.0006 and therefore matched the trends of

2/3 of the time period. The model overestimated the middle period and under estimated the latter

period significantly. However, the outcome is not surprising given the trend lines of the

observed data. The model does time the spring runoff peaks well and the peak amounts seem

reasonable when compared to the other model runs.

$$E = 1 - \frac{\sum_{t=1}^{T}(Q_o^t - Q_m^t)^2}{\sum_{t=1}^{T}(Q_o^t - \overline{Q_o})^2} \qquad (4)$$

The Nash-Sutcliffe Efficiency Coefficient (NSE), Nash and Sutcliffe (1970), method was

utilized to better estimate the accuracy of each of the model runs. NSE compares model outputs

to the observed data using equation 1. In Equation 1, Q_o^t represents the observed flow at a given

time step, Q_m^t represents the model output at the same time step, and $\overline{Q_o}$ represents the mean

observed data value. NSE values can vary from $-\infty$ to 1. In this case, 1 represents the optimum

score, meaning perfect accuracy. A score of 0 means the model performs as well as the observed

average value. NSE values were calculated for each of the three model runs both for each

individual section and the entire time window. Results are shown in Table 6 below.

Table 6. NSE model run values.

Model Run	Calibration Sections	Overall Model
1998-2003	*0.721672626*	*0.252822476*
2004-2009	0.631488348	-1.623001274
2010-2013	0.680322629	-0.525311794

The NSE values for the calibration model runs show that each of the calibration runs

performed well as each of them are close to the optimum value of 1. When comparing the

models against one another, the highest scoring calibration run was from the 1998-2003

calibration run, 0.7217, while the lowest score was from the 2004-2009 model, 0.6315.

Following suit, the highest scoring long term model run was also the 1998-2003 model with a

score of 0.2582. Also of note, the 2004-2009 model performed the poorest in the long term

model run, -1.623, due to the calibration period having a negative sloped trend line based on

observed values. Thus, resulting in poor accuracy over the long term model which has an

average positive slope, 0.001.

CHAPTER V

DISCUSSION

Soil moisture data can be powerful information, especially in the Upper Great Plains. As was discussed in previous chapters, soil moisture is a driving force in the local and regional hydrologic cycle. Over a long time period the soil moisture pattern depicts the type of ecosystems within a region and from a socio-economic stand point, the type of agricultural crops grown regionally. However, even throughout a hydrologic year, the soil moisture pattern can have an effect. A good estimation of soil moisture availability heading into an agricultural growing season could vastly improve crop yields by allowing the producers to select the proper crop genetics for the upcoming season. It was discussed that soil moisture can also influence atmospheric convective activity locally through evapotranspiration. These types of data coupled with meteorological forecast models have the potential to yield large dividends within both the agriculture and science communities. Accurately forecasting soil moisture over a period of 1-3 months would enhance, specifically, the hydrologic and atmospheric sciences in capabilities and model accuracy given the importance of soil moisture to those fields.

This study demonstrated one use of this NASA data set. However, it also revealed that hydrologic community has an opportunity to greater enhance the standard hydrologic tool set by including soil moisture as, not only an initialization data set, but an important piece of time-series data when conducting hydrologic modeling.

Also, it was noted earlier that the late summer/fall precipitation amounts were significantly greater during the 2010 – 2013 lake level period. This is also the period with the greatest lake level increases due to spring runoff. This was also the period that had the largest lake inflows during the spring runoff. The lake level period of 2010-2013 had monthly precipitation values of 2.41 and 2.73 inches for September and October, respectively, while the next closest precipitation values were 2.18 and 1.67 inches from the 2004-2009 period. However, it is possible that there were large single events late in the fall season, not seen through the averaged values, that could result in higher surface storage volume prior to freeze up.

The temperature and precipitation data do not seem to support the curious case of the downward lake level trend during the 2004-2009 period. The average temperature during that period was lowest of the three periods at 36.82 degrees F compared to 38.51 degrees F during the 2010-2013 period. Also, the precipitation during the 2004-2009 period runs the middle of the pack. However, the monthly precipitation values for June and July are up to an inch less. It is possible that rain during June and July holds more significance than previously thought. Outside of this anomaly, the temperature and precipitation statistics trend upward in the same fashion as the 1998-2003 and 2010-2013 time periods.

Temperature and precipitation data are shown in Appendix B. Munna (2012) discussed the difference in hydrologic effects of large precipitation events. Although, it is possible for the ground gages to misrepresent large rain events, it was shown in this study that the spring time runoff was more important than the large rain events.

The largest inflows into the lake were observed during the spring runoff. It is intuitive, then, that the years of the highest inflows from melt runoff would coincide with the years of the

highest precipitation. For this study, it was assumed that 'winter' was November to March. The period of 2004-2009 split the precipitation values of the other two periods for all of the months except November. During the month of November the average 2004-2009 precipitation was highest of the three periods with 0.81 inches compared to 0.72 and 0.79 inches. When comparing the temperatures in similar fashion, it was found that the 2004-2009 November average was the highest, December average the lowest, and the rest to lie in the middle. Again, the statistics did not point to an obvious climate scenario leading to the downward trend in lake levels. Thus, the model does not recognize the hydrologic changes within the basin given the climate parameters introduced into the model and does not adjust to the periodicity of natural environment in this case. However, it is possible that there are variables missing from the current calibrated model.

The variables within this model were averaged over each subbasin. The separation of upland storage capacities and wetland storage capacities within each subbasin is one possible enhancement to the current approach. Also, calculation of additional variables that can be held static within the model would allow for additional knowledge of unknown parameter, such as seepage and horizontal groundwater flow.

CHAPTER VI

CONCLUSIONS

The outcomes of this research describe the capabilities of HEC-HMS to handle a

reservoir model using the soil moisture and accounting loss method which includes soil moisture

data. The path to reach these outcomes started with the modification of a previous model,

Munna (2012) and Hassel (2010), to one that utilized the soil moisture accounting loss approach.

Once the revamped model was operational, the sensitivity analysis was performed to better

understand the influences each variable had on the model outcomes. Finally, the model was

adjusted to fit the observed lake levels for Devils Lake.

The hypothesis was that the spatial volumetric soil moisture data, specifically NASA's

LPRM daily soil moisture data, would increase the accuracy of a hydrologic model that had

originally been built using constant loss values. Munna (2012) stated that the previous model,

which had two model runs, had root mean squared errors (RMSE) of 1.49 ft and 1.73 ft,

respectively. That model used a window of 2003-2010 for its operational period. As shown in

this research, that time frame coincides with two separate hydrologic patterns in the basin. The

2004-2009 model using SMA parameters from this current study most closely fits that window,

and had a RMSE of 0.85 ft. However, the SMA method produced better results during the two

other lake level regimes, 1998-2003 and 2010-2013. The 1998-2003 and 2010-2013 models

produced RMSE values of -0.412 ft and -.387 ft, respectively. When the 1998-2003, 2004-2009,

and 2010-2013 calibration models were applied individually to the 1998-2013 window they

produced RMSE values of -2.299, 2.009, and -2.314, respectively. The variation from the short term calibration RMSE values to the long term RMSE values was caused by differences in the observed lake level trends of the three time periods. The model, when given a specific set of parameters, was unable to replicate significant environmental changes influencing observed lake level trends. Also, over the 1998-2013 window the model did a good job of replicating the overall observed data when comparing the starting lake level to the ending lake level.

Previous research has shown that the opportunity to include soil moisture into hydrologic models can be a powerful tool. However, in the case of HEC-HMS, the inability of the model to use the daily recorded time series data in the same fashion it utilizes temperature or precipitation significantly reduces the models capabilities. One solution to this maybe to increase the occasions for which the original HEC-HMS formula is used, allowing adjustment of parameters on the fly relative to the observed data trends.

APPENDICES

A. HEC-HMS SOIL MOISTURE ACCOUNTING PARAMETERS

Table 7. SMA Parameters 2010-2013

Subbasin	Canopy %	Surface %	Soil %	Canopy Stor IN	Surface Stor IN	Max Infil IN/HR	Impervious %	Soil Stor IN	Tension Stor IN	Soil Perc IN/HR
4_M-4	20	20	20	0	0.1	0.3992055	8	0.15	0.1	0.05
3_M-3	20	20	20	0	0.1	0.48155	8	0.15	0.1	0.05
2_M-2	20	20	20	0	0.1	0.439843	8	0.15	0.1	0.05
7_M-7	20	20	20	0	0.1	0.414881	8	0.15	0.1	0.05
17_M-17	20	20	20	0	0.1	0.3234385	8	0.15	0.1	0.05
1_M-1	20	20	20	0	0.1	0.65194	8	0.15	0.1	0.05
12_M-12	20	20	20	0	0.1	0.432724	8	0.15	0.1	0.05
6_M-6	20	20	20	0	0.1	0.41301	8	0.15	0.1	0.05
5_M-5	20	20	20	0	0.1	0.51881	8	0.15	0.1	0.05
10_M-10	20	20	20	0	0.1	0.4738245	8	0.15	0.1	0.05
9_M-9	20	20	20	0	0.1	0.55761	8	0.15	0.1	0.05
13_M-13	20	20	20	0	0.1	0.343936	8	0.15	0.1	0.05
8_M-8	20	20	20	0	0.1	0.407799	8	0.15	0.1	0.05
18_M-18	20	20	20	0	0.1	0.61008	8	0.15	0.1	0.05
11_M-11	20	20	20	0	0.1	0.563571	8	0.15	0.1	0.05
20_M-20	20	20	20	0	0.1	0.414881	8	0.15	0.1	0.05
14_M-14	20	20	20	0	0.1	0.3593915	8	0.15	0.1	0.05
15_M-15	20	20	20	0	0.1	0.36176	8	0.15	0.1	0.05
16_M-16	20	20	20	0	0.1	0.4288775	8	0.15	0.1	0.05
19_M-19	20	20	20	0	0.1	0.439843	8	0.15	0.1	0.05
47_E-2	20	20	20	0	0.1	0.79795	8	0.15	0.1	0.05
46_E-1	20	20	20	0	0.1	0.6134	8	0.15	0.1	0.05
48_E-3	20	20	20	0	0.1	0.71405	8	0.15	0.1	0.05
49_E-4	20	20	20	0	0.1	0.71405	8	0.15	0.1	0.05
53_E-8	20	20	20	0	0.1	0.6197	8	0.15	0.1	0.05
51_E-6	20	20	20	0	0.1	0.64425	8	0.15	0.1	0.05
52_E-7	20	20	20	0	0.1	0.71405	8	0.15	0.1	0.05
50_E-5	20	20	20	0	0.1	0.53045	8	0.15	0.1	0.05
54_E-9	20	20	20	0	0.1	0.64425	8	0.15	0.1	0.05
56_E-11	20	20	20	0	0.1	0.51475	8	0.15	0.1	0.05
57_E-12	20	20	20	0	0.1	0.56435	8	0.15	0.1	0.05
55_E-10	20	20	20	0	0.1	0.5327	8	0.15	0.1	0.05
60_E-15	20	20	20	0	0.1	0.55535	8	0.15	0.1	0.05
58_E-13	20	20	20	0	0.1	0.56555	8	0.15	0.1	0.05
59_E-14	20	20	20	0	0.1	0.5908	8	0.15	0.1	0.05
63_L-3	20	20	20	0	0.1	1.22555	8	0.15	0.1	0.05
62_L-2	20	20	20	0	0.1	1.22555	8	0.15	0.1	0.05
61_L-1	20	20	20	0	0.1	1.22555	8	0.15	0.1	0.05
65_L-5	20	20	20	0	0.1	0.5198	8	0.15	0.1	0.05
64_L-4	20	20	20	0	0.1	0.5198	8	0.15	0.1	0.05
69_L-9	20	20	20	0	0.1	0.63975	8	0.15	0.1	0.05
66_L-6	20	20	20	0	0.1	0.5828	8	0.15	0.1	0.05
67_L-7	20	20	20	0	0.1	0.7245	8	0.15	0.1	0.05
68_L-8	20	20	20	0	0.1	0.5972	8	0.15	0.1	0.05
72_L-12	20	20	20	0	0.1	0.5972	8	0.15	0.1	0.05

Table 7 cont

73_L-13	20	20	20	0	0.1	0.746	8	0.15	0.1	0.05
70_L-10	20	20	20	0	0.1	0.6668	8	0.15	0.1	0.05
71_L-11	20	20	20	0	0.1	0.5987	8	0.15	0.1	0.05
96_DN-1	20	20	20	0	0.1	0.6	8	0.15	0.1	0.05
97_DS-1	20	20	20	0	0.1	0.6	8	0.15	0.1	0.05
75_S-2	20	20	20	0	0.1	0.6197	8	0.15	0.1	0.05
74_S-1	20	20	20	0	0.1	0.6197	8	0.15	0.1	0.05
77_S-4	20	20	20	0	0.1	0.6197	8	0.15	0.1	0.05
79_S-6	20	20	20	0	0.1	0.5565	8	0.15	0.1	0.05
80_S-7	20	20	20	0	0.1	0.5565	8	0.15	0.1	0.05
82_S-9	20	20	20	0	0.1	0.5565	8	0.15	0.1	0.05
85_S-12	20	20	20	0	0.1	0.53915	8	0.15	0.1	0.05
84_S-11	20	20	20	0	0.1	0.5881	8	0.15	0.1	0.05
91_S-18	20	20	20	0	0.1	0.5619	8	0.15	0.1	0.05
90_S-17	20	20	20	0	0.1	0.5619	8	0.15	0.1	0.05
92_S-19	20	20	20	0	0.1	0.6307	8	0.15	0.1	0.05
78_S-5	20	20	20	0	0.1	0.53915	8	0.15	0.1	0.05
76_S-3	20	20	20	0	0.1	0.53915	8	0.15	0.1	0.05
83_S-10	20	20	20	0	0.1	0.53915	8	0.15	0.1	0.05
81_S-8	20	20	20	0	0.1	0.53915	8	0.15	0.1	0.05
86_S-13	20	20	20	0	0.1	0.53915	8	0.15	0.1	0.05
88_S-15	20	20	20	0	0.1	0.65325	8	0.15	0.1	0.05
89_S-16	20	20	20	0	0.1	0.5619	8	0.15	0.1	0.05
87_S-14	20	20	20	0	0.1	0.65325	8	0.15	0.1	0.05
31_W-2	20	20	20	0	0.1	0.569	8	0.15	0.1	0.05
30_W-1	20	20	20	0	0.1	0.569	8	0.15	0.1	0.05
37_W-8	20	20	20	0	0.1	0.64455	8	0.15	0.1	0.05
32_W-3	20	20	20	0	0.1	0.54225	8	0.15	0.1	0.05
34_W-5	20	20	20	0	0.1	0.51475	8	0.15	0.1	0.05
33_W-4	20	20	20	0	0.1	0.575	8	0.15	0.1	0.05
36_W-7	20	20	20	0	0.1	0.7011	8	0.15	0.1	0.05
38_W-9	20	20	20	0	0.1	0.7011	8	0.15	0.1	0.05
39_W-10	20	20	20	0	0.1	0.7011	8	0.15	0.1	0.05
41_W-12	20	20	20	0	0.1	1.0112	8	0.15	0.1	0.05
35_W-6	20	20	20	0	0.1	0.65945	8	0.15	0.1	0.05
42_W-13	20	20	20	0	0.1	0.65945	8	0.15	0.1	0.05
40_W-11	20	20	20	0	0.1	1.0112	8	0.15	0.1	0.05
45_W-16	20	20	20	0	0.1	1.0112	8	0.15	0.1	0.05
43_W-14	20	20	20	0	0.1	1.0112	8	0.15	0.1	0.05
44_W-15	20	20	20	0	0.1	0.52438	8	0.15	0.1	0.05
21_C-1	20	20	20	0	0.1	0.8497	8	0.15	0.1	0.05
22_C-2	20	20	20	0	0.1	0.66515	8	0.15	0.1	0.05
24_C-4	20	20	20	0	0.1	0.78765	8	0.15	0.1	0.05
26_C-6	20	20	20	0	0.1	1.0145	8	0.15	0.1	0.05
23_C-3	20	20	20	0	0.1	0.69525	8	0.15	0.1	0.05
25_C-5	20	20	20	0	0.1	1.15395	8	0.15	0.1	0.05
27_C-7	20	20	20	0	0.1	1.15395	8	0.15	0.1	0.05
28_C-8	20	20	20	0	0.1	1.2767	8	0.15	0.1	0.05
29_C-9	20	20	20	0	0.1	1.2767	8	0.15	0.1	0.05
93_S-20	20	20	20	0	0.1	0.57995	8	0.15	0.1	0.05
94_S-21	20	20	20	0	0.1	0.5424	8	0.15	0.1	0.05
95_S-22	20	20	20	0	0.1	0.57995	8	0.15	0.1	0.05

Table 8. SMA Parameters 2004-2009.

Subbasin	Canopy %	Surface %	Soil %	Canopy Stor IN	Surface Stor IN	Max Infil IN/HR	Impervious %	Soil Stor IN	Tension Stor IN	Soil Perc IN/HR
4_M-4	20	20	20	0.2	0.2	0.3992055	8	0.2	0.15	0.1
3_M-3	20	20	20	0.2	0.2	0.48155	8	0.2	0.15	0.1
2_M-2	20	20	20	0.2	0.2	0.439843	8	0.2	0.15	0.1
7_M-7	20	20	20	0.2	0.2	0.414881	8	0.2	0.15	0.1
17_M-17	20	20	20	0.2	0.2	0.3234385	8	0.2	0.15	0.1
1_M-1	20	20	20	0.2	0.2	0.65194	8	0.2	0.15	0.1
12_M-12	20	20	20	0.2	0.2	0.432724	8	0.2	0.15	0.1
6_M-6	20	20	20	0.2	0.2	0.41301	8	0.2	0.15	0.1
5_M-5	20	20	20	0.2	0.2	0.51881	8	0.2	0.15	0.1
10_M-10	20	20	20	0.2	0.2	0.4738245	8	0.2	0.15	0.1
9_M-9	20	20	20	0.2	0.2	0.55761	8	0.2	0.15	0.1
13_M-13	20	20	20	0.2	0.2	0.343936	8	0.2	0.15	0.1
8_M-8	20	20	20	0.2	0.2	0.407799	8	0.2	0.15	0.1
18_M-18	20	20	20	0.2	0.2	0.61008	8	0.2	0.15	0.1
11_M-11	20	20	20	0.2	0.2	0.563571	8	0.2	0.15	0.1
20_M-20	20	20	20	0.2	0.2	0.414881	8	0.2	0.15	0.1
14_M-14	20	20	20	0.2	0.2	0.3593915	8	0.2	0.15	0.1
15_M-15	20	20	20	0.2	0.2	0.36176	8	0.2	0.15	0.1
16_M-16	20	20	20	0.2	0.2	0.4288775	8	0.2	0.15	0.1
19_M-19	20	20	20	0.2	0.2	0.439843	8	0.2	0.15	0.1
47_E-2	20	20	20	0.2	0.2	0.79795	8	0.2	0.15	0.1
46_E-1	20	20	20	0.2	0.2	0.6134	8	0.2	0.15	0.1
48_E-3	20	20	20	0.2	0.2	0.71405	8	0.2	0.15	0.1
49_E-4	20	20	20	0.2	0.2	0.71405	8	0.2	0.15	0.1
53_E-8	20	20	20	0.2	0.2	0.6197	8	0.2	0.15	0.1
51_E-6	20	20	20	0.2	0.2	0.64425	8	0.2	0.15	0.1
52_E-7	20	20	20	0.2	0.2	0.71405	8	0.2	0.15	0.1
50_E-5	20	20	20	0.2	0.2	0.53045	8	0.2	0.15	0.1
54_E-9	20	20	20	0.2	0.2	0.64425	8	0.2	0.15	0.1
56_E-11	20	20	20	0.2	0.2	0.51475	8	0.2	0.15	0.1
57_E-12	20	20	20	0.2	0.2	0.56435	8	0.2	0.15	0.1
55_E-10	20	20	20	0.2	0.2	0.5327	8	0.2	0.15	0.1
60_E-15	20	20	20	0.2	0.2	0.55535	8	0.2	0.15	0.1
58_E-13	20	20	20	0.2	0.2	0.56555	8	0.2	0.15	0.1
59_E-14	20	20	20	0.2	0.2	0.5908	8	0.2	0.15	0.1
63_L-3	20	20	20	0.2	0.2	1.22555	8	0.2	0.15	0.1
62_L-2	20	20	20	0.2	0.2	1.22555	8	0.2	0.15	0.1
61_L-1	20	20	20	0.2	0.2	1.22555	8	0.2	0.15	0.1
65_L-5	20	20	20	0.2	0.2	0.5198	8	0.2	0.15	0.1
64_L-4	20	20	20	0.2	0.2	0.5198	8	0.2	0.15	0.1
69_L-9	20	20	20	0.2	0.2	0.63975	8	0.2	0.15	0.1
66_L-6	20	20	20	0.2	0.2	0.5828	8	0.2	0.15	0.1
67_L-7	20	20	20	0.2	0.2	0.7245	8	0.2	0.15	0.1
68_L-8	20	20	20	0.2	0.2	0.5972	8	0.2	0.15	0.1
72_L-12	20	20	20	0.2	0.2	0.5972	8	0.2	0.15	0.1
73_L-13	20	20	20	0.2	0.2	0.746	8	0.2	0.15	0.1
70_L-10	20	20	20	0.2	0.2	0.6668	8	0.2	0.15	0.1
71_L-11	20	20	20	0.2	0.2	0.5987	8	0.2	0.15	0.1
96_DN-1	20	20	20	0.2	0.2	0.6	8	0.2	0.15	0.1
97_DS-1	20	20	20	0.2	0.2	0.6	8	0.2	0.15	0.1
75_S-2	20	20	20	0.2	0.2	0.6197	8	0.2	0.15	0.1
74_S-1	20	20	20	0.2	0.2	0.6197	8	0.2	0.15	0.1

Table 8 cont.

77_S-4	20	20	20	0.2	0.2	0.6197	8	0.2	0.15	0.1
79_S-6	20	20	20	0.2	0.2	0.5565	8	0.2	0.15	0.1
80_S-7	20	20	20	0.2	0.2	0.5565	8	0.2	0.15	0.1
82_S-9	20	20	20	0.2	0.2	0.5565	8	0.2	0.15	0.1
85_S-12	20	20	20	0.2	0.2	0.53915	8	0.2	0.15	0.1
84_S-11	20	20	20	0.2	0.2	0.5881	8	0.2	0.15	0.1
91_S-18	20	20	20	0.2	0.2	0.5619	8	0.2	0.15	0.1
90_S-17	20	20	20	0.2	0.2	0.5619	8	0.2	0.15	0.1
92_S-19	20	20	20	0.2	0.2	0.6307	8	0.2	0.15	0.1
78_S-5	20	20	20	0.2	0.2	0.53915	8	0.2	0.15	0.1
76_S-3	20	20	20	0.2	0.2	0.53915	8	0.2	0.15	0.1
83_S-10	20	20	20	0.2	0.2	0.53915	8	0.2	0.15	0.1
81_S-8	20	20	20	0.2	0.2	0.53915	8	0.2	0.15	0.1
86_S-13	20	20	20	0.2	0.2	0.53915	8	0.2	0.15	0.1
88_S-15	20	20	20	0.2	0.2	0.65325	8	0.2	0.15	0.1
89_S-16	20	20	20	0.2	0.2	0.5619	8	0.2	0.15	0.1
87_S-14	20	20	20	0.2	0.2	0.65325	8	0.2	0.15	0.1
31_W-2	20	20	20	0.2	0.2	0.569	8	0.2	0.15	0.1
30_W-1	20	20	20	0.2	0.2	0.569	8	0.2	0.15	0.1
37_W-8	20	20	20	0.2	0.2	0.64455	8	0.2	0.15	0.1
32_W-3	20	20	20	0.2	0.2	0.54225	8	0.2	0.15	0.1
34_W-5	20	20	20	0.2	0.2	0.51475	8	0.2	0.15	0.1
33_W-4	20	20	20	0.2	0.2	0.575	8	0.2	0.15	0.1
36_W-7	20	20	20	0.2	0.2	0.7011	8	0.2	0.15	0.1
38_W-9	20	20	20	0.2	0.2	0.7011	8	0.2	0.15	0.1
39_W-10	20	20	20	0.2	0.2	0.7011	8	0.2	0.15	0.1
41_W-12	20	20	20	0.2	0.2	1.0112	8	0.2	0.15	0.1
35_W-6	20	20	20	0.2	0.2	0.65945	8	0.2	0.15	0.1
42_W-13	20	20	20	0.2	0.2	0.65945	8	0.2	0.15	0.1
40_W-11	20	20	20	0.2	0.2	1.0112	8	0.2	0.15	0.1
45_W-16	20	20	20	0.2	0.2	1.0112	8	0.2	0.15	0.1
43_W-14	20	20	20	0.2	0.2	1.0112	8	0.2	0.15	0.1
44_W-15	20	20	20	0.2	0.2	0.52438	8	0.2	0.15	0.1
21_C-1	20	20	20	0.2	0.2	0.8497	8	0.2	0.15	0.1
22_C-2	20	20	20	0.2	0.2	0.66515	8	0.2	0.15	0.1
24_C-4	20	20	20	0.2	0.2	0.78765	8	0.2	0.15	0.1
26_C-6	20	20	20	0.2	0.2	1.0145	8	0.2	0.15	0.1
23_C-3	20	20	20	0.2	0.2	0.69525	8	0.2	0.15	0.1
25_C-5	20	20	20	0.2	0.2	1.15395	8	0.2	0.15	0.1
27_C-7	20	20	20	0.2	0.2	1.15395	8	0.2	0.15	0.1
28_C-8	20	20	20	0.2	0.2	1.2767	8	0.2	0.15	0.1
29_C-9	20	20	20	0.2	0.2	1.2767	8	0.2	0.15	0.1
93_S-20	20	20	20	0.2	0.2	0.57995	8	0.2	0.15	0.1
94_S-21	20	20	20	0.2	0.2	0.5424	8	0.2	0.15	0.1
95_S-22	20	20	20	0.2	0.2	0.57995	8	0.2	0.15	0.1

Table 9. SMA Parameters 1998-2003.

Subbasin	Canopy %	Surface %	Soil %	Canopy Stor IN	Surface Stor IN	Max Infil IN/HR	Impervious %	Soil Stor IN	Tension Stor IN	Soil Perc IN/HR
4_M-4	20	100	20	0	0	0.3992055	10	0.15	0.05	0.15
3_M-3	20	100	20	0	0	0.48155	10	0.15	0.05	0.15

Table 9 cont.

2_M-2	20	100	20	0	0	0.439843	10	0.15	0.05	0.15
7_M-7	20	100	20	0	0	0.414881	10	0.15	0.05	0.15
17_M-17	20	100	20	0	0	0.3234385	10	0.15	0.05	0.15
1_M-1	20	100	20	0	0	0.65194	10	0.15	0.05	0.15
12_M-12	20	100	20	0	0	0.432724	10	0.15	0.05	0.15
6_M-6	20	100	20	0	0	0.41301	10	0.15	0.05	0.15
5_M-5	20	100	20	0	0	0.51881	10	0.15	0.05	0.15
10_M-10	20	100	20	0	0	0.4738245	10	0.15	0.05	0.15
9_M-9	20	100	20	0	0	0.55761	10	0.15	0.05	0.15
13_M-13	20	100	20	0	0	0.343936	10	0.15	0.05	0.15
8_M-8	20	100	20	0	0	0.407799	10	0.15	0.05	0.15
18_M-18	20	100	20	0	0	0.61008	10	0.15	0.05	0.15
11_M-11	20	100	20	0	0	0.563571	10	0.15	0.05	0.15
20_M-20	20	100	20	0	0	0.414881	10	0.15	0.05	0.15
14_M-14	20	100	20	0	0	0.3593915	10	0.15	0.05	0.15
15_M-15	20	100	20	0	0	0.36176	10	0.15	0.05	0.15
16_M-16	20	100	20	0	0	0.4288775	10	0.15	0.05	0.15
19_M-19	20	100	20	0	0	0.439843	10	0.15	0.05	0.15
47_E-2	20	100	20	0	0	0.79795	10	0.15	0.05	0.15
46_E-1	20	100	20	0	0	0.6134	10	0.15	0.05	0.15
48_E-3	20	100	20	0	0	0.71405	10	0.15	0.05	0.15
49_E-4	20	100	20	0	0	0.71405	10	0.15	0.05	0.15
53_E-8	20	100	20	0	0	0.6197	10	0.15	0.05	0.15
51_E-6	20	100	20	0	0	0.64425	10	0.15	0.05	0.15
52_E-7	20	100	20	0	0	0.71405	10	0.15	0.05	0.15
50_E-5	20	100	20	0	0	0.53045	10	0.15	0.05	0.15
54_E-9	20	100	20	0	0	0.64425	10	0.15	0.05	0.15
56_E-11	20	100	20	0	0	0.51475	10	0.15	0.05	0.15
57_E-12	20	100	20	0	0	0.56435	10	0.15	0.05	0.15
55_E-10	20	100	20	0	0	0.5327	10	0.15	0.05	0.15
60_E-15	20	100	20	0	0	0.55535	10	0.15	0.05	0.15
58_E-13	20	100	20	0	0	0.56555	10	0.15	0.05	0.15
59_E-14	20	100	20	0	0	0.5908	10	0.15	0.05	0.15
63_L-3	20	100	20	0	0	1.22555	10	0.15	0.05	0.15
62_L-2	20	100	20	0	0	1.22555	10	0.15	0.05	0.15
61_L-1	20	100	20	0	0	1.22555	10	0.15	0.05	0.15
65_L-5	20	100	20	0	0	0.5198	10	0.15	0.05	0.15
64_L-4	20	100	20	0	0	0.5198	10	0.15	0.05	0.15
69_L-9	20	100	20	0	0	0.63975	10	0.15	0.05	0.15
66_L-6	20	100	20	0	0	0.5828	10	0.15	0.05	0.15
67_L-7	20	100	20	0	0	0.7245	10	0.15	0.05	0.15
68_L-8	20	100	20	0	0	0.5972	10	0.15	0.05	0.15
72_L-12	20	100	20	0	0	0.5972	10	0.15	0.05	0.15
73_L-13	20	100	20	0	0	0.746	10	0.15	0.05	0.15
70_L-10	20	100	20	0	0	0.6668	10	0.15	0.05	0.15
71_L-11	20	100	20	0	0	0.5987	10	0.15	0.05	0.15
96_DN-1	20	100	20	0	0	0.6	10	0.15	0.05	0.15
97_DS-1	20	100	20	0	0	0.6	10	0.15	0.05	0.15
75_S-2	20	100	20	0	0	0.6197	10	0.15	0.05	0.15
74_S-1	20	100	20	0	0	0.6197	10	0.15	0.05	0.15
77_S-4	20	100	20	0	0	0.6197	10	0.15	0.05	0.15
79_S-6	20	100	20	0	0	0.5565	10	0.15	0.05	0.15
80_S-7	20	100	20	0	0	0.5565	10	0.15	0.05	0.15
82_S-9	20	100	20	0	0	0.5565	10	0.15	0.05	0.15

Table 9 cont.

85_S-12	20	100	20	0	0	0.53915	10	0.15	0.05	0.15
84_S-11	20	100	20	0	0	0.5881	10	0.15	0.05	0.15
91_S-18	20	100	20	0	0	0.5619	10	0.15	0.05	0.15
90_S-17	20	100	20	0	0	0.5619	10	0.15	0.05	0.15
92_S-19	20	100	20	0	0	0.6307	10	0.15	0.05	0.15
78_S-5	20	100	20	0	0	0.53915	10	0.15	0.05	0.15
76_S-3	20	100	20	0	0	0.53915	10	0.15	0.05	0.15
83_S-10	20	100	20	0	0	0.53915	10	0.15	0.05	0.15
81_S-8	20	100	20	0	0	0.53915	10	0.15	0.05	0.15
86_S-13	20	100	20	0	0	0.53915	10	0.15	0.05	0.15
88_S-15	20	100	20	0	0	0.65325	10	0.15	0.05	0.15
89_S-16	20	100	20	0	0	0.5619	10	0.15	0.05	0.15
87_S-14	20	100	20	0	0	0.65325	10	0.15	0.05	0.15
31_W-2	20	100	20	0	0	0.569	10	0.15	0.05	0.15
30_W-1	20	100	20	0	0	0.569	10	0.15	0.05	0.15
37_W-8	20	100	20	0	0	0.64455	10	0.15	0.05	0.15
32_W-3	20	100	20	0	0	0.54225	10	0.15	0.05	0.15
34_W-5	20	100	20	0	0	0.51475	10	0.15	0.05	0.15
33_W-4	20	100	20	0	0	0.575	10	0.15	0.05	0.15
36_W-7	20	100	20	0	0	0.7011	10	0.15	0.05	0.15
38_W-9	20	100	20	0	0	0.7011	10	0.15	0.05	0.15
39_W-10	20	100	20	0	0	0.7011	10	0.15	0.05	0.15
41_W-12	20	100	20	0	0	1.0112	10	0.15	0.05	0.15
35_W-6	20	100	20	0	0	0.65945	10	0.15	0.05	0.15
42_W-13	20	100	20	0	0	0.65945	10	0.15	0.05	0.15
40_W-11	20	100	20	0	0	1.0112	10	0.15	0.05	0.15
45_W-16	20	100	20	0	0	1.0112	10	0.15	0.05	0.15
43_W-14	20	100	20	0	0	1.0112	10	0.15	0.05	0.15
44_W-15	20	100	20	0	0	0.52438	10	0.15	0.05	0.15
21_C-1	20	100	20	0	0	0.8497	10	0.15	0.05	0.15
22_C-2	20	100	20	0	0	0.66515	10	0.15	0.05	0.15
24_C-4	20	100	20	0	0	0.78765	10	0.15	0.05	0.15
26_C-6	20	100	20	0	0	1.0145	10	0.15	0.05	0.15
23_C-3	20	100	20	0	0	0.69525	10	0.15	0.05	0.15
25_C-5	20	100	20	0	0	1.15395	10	0.15	0.05	0.15
27_C-7	20	100	20	0	0	1.15395	10	0.15	0.05	0.15
28_C-8	20	100	20	0	0	1.2767	10	0.15	0.05	0.15
29_C-9	20	100	20	0	0	1.2767	10	0.15	0.05	0.15
93_S-20	20	100	20	0	0	0.57995	10	0.15	0.05	0.15
94_S-21	20	100	20	0	0	0.5424	10	0.15	0.05	0.15
95_S-22	20	100	20	0	0	0.57995	10	0.15	0.05	0.15

B. CLIMATE DATA

Table 10. Precipitation Data

Year	Jan	Feb	Mar	Apr	May	Jun	Jul	Aug	Sep	Oct	Nov	Dec	Total	
														Ave
1998							1.32	0.40	0.30	2.80	0.60	0.10	5.52	Total
1999	0.40	0.40	0.40	0.90	4.60	3.00	3.40	1.90	1.20	0.00	0.10	0.40	16.70	1999-2003

Table 10 cont.

Year	Jan	Feb	Mar	Apr	May	Jun	Jul	Aug	Sep	Oct	Nov	Dec	Total	
2000	0.10	0.80	0.70	0.20	1.80	4.40	2.30	4.70	1.20	1.10	3.00	0.60	20.90	1.36
2001	0.00	0.10	0.10	1.90	2.29	5.31	4.40	1.00	0.90	1.20	0.20	0.40	17.80	
2002	0.10	0.00	0.20	0.50	1.00	6.30	1.50	1.67	1.53	0.50	0.00	0.40	13.70	
2003	0.20	0.10	0.70	0.90	1.00	3.60	2.10	1.70	1.30	0.20	0.30	0.50	12.60	
														2004-2009
2004	0.90	0.20	2.20	1.60	6.09	1.51	2.39	3.31	3.20	1.20	0.00	0.60	23.20	
2005	0.70	0.00	0.50	1.30	3.29	5.81	1.10	3.30	0.50	1.70	1.30	0.40	19.90	1.69
2006	0.80	0.50	1.20	1.49	1.71	1.59	2.21	3.70	1.70	0.70	0.60	0.70	16.90	
2007	0.00	0.69	2.09	0.03	5.70	4.40	4.89	0.71	0.80	1.30	0.40	0.60	21.60	
2008	0.10	0.30	0.40	1.00	0.90	4.60	2.30	1.50	3.60	2.90	2.54	0.65	20.79	
														2010-2013
2009	0.19	0.69	0.93	1.39	2.37	4.07	1.20	1.70	3.29	2.21	0.00	0.90	18.94	
2010	0.40	0.20	1.30	3.00	3.30	2.80	3.40	1.40	4.70	0.80	0.00	0.00	21.30	2.24
2011	0.67	0.19	0.44	1.63	2.67	4.68	4.28	3.53	2.15	1.37	0.32	0.39	22.32	
2012	0.92	0.44	1.13	1.22	4.46	4.77	3.37	3.15	0.70	4.51	1.86	1.19	27.73	
2013	1.22	1.35	2.31	1.34	10.13	4.81	3.28	1.27	2.09	4.25	0.99	2.92	35.96	
Total	6.69	5.96	14.60	18.39	51.30	61.67	43.43	34.96	29.16	26.73	12.21	10.75	315.85	

Monthly Ave	Jan	Feb	Mar	Apr	May	Jun	Jul	Aug	Sep	Oct	Nov	Dec
1999-2003	0.16	0.28	0.42	0.88	2.14	4.52	2.74	2.20	1.23	0.60	0.72	0.46
2004-2009	0.45	0.40	1.22	1.13	3.34	3.66	2.35	2.37	2.18	1.67	0.81	0.64
2010-2013	0.80	0.55	1.29	1.80	5.14	4.27	3.58	2.34	2.41	2.73	0.79	1.12

Table 11. Temperature Data.

Year	Jan	Feb	Mar	Apr	May	Jun	Jul	Aug	Sep	Oct	Nov	Dec	Ave	Yearly Aver
1998							66.63	68.12	59.49	42.67	23.98	10.65	45.18	
1999	-0.62	15.80	25.44	40.95	52.82	60.70	66.18	63.73	52.59	38.84	33.29	18.72	39.14	1999-2003
2000	5.42	18.62	32.00	38.39	53.34	57.18	66.11	65.83	55.45	43.06	20.32	-4.21	37.67	37.46
2001	10.30	-0.16	20.25	38.67	54.22	60.15	67.16	67.61	55.42	38.37	34.14	13.68	38.54	
2002	9.71	15.35	10.75	35.31	45.28	63.19	68.67	67.73	56.87	31.23	23.17	16.13	37.04	
2003	4.04	0.29	16.96	40.64	45.23	61.56	66.53	56.84	55.19	44.36	17.05	15.87	35.58	2004-2009
2004	-4.73	9.92	21.82	38.46	45.46	57.09	64.13	56.77	57.07	41.20	30.60	11.09	35.77	36.82
2005	-0.90	10.71	19.23	44.24	48.99	57.09	66.49	63.46	57.52	43.33	27.28	14.83	37.81	
2006	19.80	4.82	21.10	45.48	52.87	64.45	69.79	66.32	54.62	37.91	24.04	16.09	39.98	
2007	6.34	4.82	22.69	39.43	52.61	63.49	69.63	63.04	54.83	43.90	24.79	5.94	37.81	
2008	2.66	1.55	17.97	37.40	48.41	59.74	64.90	63.09	54.99	42.47	24.77	-1.42	34.79	2010-2013
2009	-2.87	4.87	14.72	35.26	47.72	59.82	63.10	63.01	63.07	37.86	34.20	3.73	35.49	38.51
2010	7.61	7.28	30.56	47.00	53.10	62.43	67.93	67.61	53.98	46.35	25.23	6.15	39.79	
2011	1.30	6.03	16.40	37.45	51.21	62.61	69.34	66.27	56.17	47.39	27.63	20.38	38.70	
2012	15.23	14.43	36.95	43.91	54.70	64.21	70.90	65.55	55.02	38.81	21.57	7.93	40.85	
2013	5.21	10.41	9.58	24.29	51.69	64.58	66.79	66.70	59.94	40.31	22.67	-0.55	35.35	
Total	5.23	8.34	21.09	39.12	50.51	61.22	67.14	64.48	56.39	41.13	25.92	9.71	37.86	

Monthly Ave	Jan	Feb	Mar	Apr	May	Jun	Jul	Aug	Sep	Oct	Nov	Dec
1999-2003	5.77	9.98	21.08	38.79	50.18	60.55	66.93	64.35	55.10	39.17	25.60	12.04
2004-2009	3.48	5.28	19.21	40.13	48.76	60.46	66.37	61.79	56.75	41.58	26.11	9.45
2010-2013	7.34	9.54	23.37	38.16	52.68	63.46	68.74	66.53	56.28	43.21	24.27	8.48

C. NASA DATA

http://hydro1.sci.gsfc.nasa.gov/opendap/hyrax/ncml/LPRM_AMSRE_D_SOILM3_timeSeries.nc
ml.ascii?soil_moisture_c[0:1:336][320:320][168:168]

Dataset: LPRM_AMSRE_D_SOILM3_timeSeries.ncml

soil_moisture_c.Latitude, 47.875

soil_moisture_c.soil_moisture_c[soil_moisture_c.time="2002-06-19T00:00:00Z"][soil_moisture_c.Longitude=-99.875], 31

soil_moisture_c.soil_moisture_c[soil_moisture_c.time="2002-06-20T00:00:00Z"][soil_moisture_c.Longitude=-99.875], -32767

soil_moisture_c.soil_moisture_c[soil_moisture_c.time="2002-06-21T00:00:00Z"][soil_moisture_c.Longitude=-99.875], 26

soil_moisture_c.soil_moisture_c[soil_moisture_c.time="2002-06-22T00:00:00Z"][soil_moisture_c.Longitude=-99.875], 21

soil_moisture_c.soil_moisture_c[soil_moisture_c.time="2002-06-23T00:00:00Z"][soil_moisture_c.Longitude=-99.875], 28

soil_moisture_c.soil_moisture_c[soil_moisture_c.time="2002-06-24T00:00:00Z"][soil_moisture_c.Longitude=-99.875], 35

soil_moisture_c.soil_moisture_c[soil_moisture_c.time="2002-06-25T00:00:00Z"][soil_moisture_c.Longitude=-99.875], 27

soil_moisture_c.soil_moisture_c[soil_moisture_c.time="2002-06-26T00:00:00Z"][soil_moisture_c.Longitude=-99.875], 26

soil_moisture_c.soil_moisture_c[soil_moisture_c.time="2002-06-27T00:00:00Z"][soil_moisture_c.Longitude=-99.875], -32767

soil_moisture_c.soil_moisture_c[soil_moisture_c.time="2002-06-28T00:00:00Z"][soil_moisture_c.Longitude=-99.875], -32767

soil_moisture_c.soil_moisture_c[soil_moisture_c.time="2002-06-29T00:00:00Z"][soil_moisture_c.Longitude=-99.875], -32767

soil_moisture_c.soil_moisture_c[soil_moisture_c.time="2002-06-30T00:00:00Z"][soil_moisture_c.Longitude=-99.875], 25

soil_moisture_c.soil_moisture_c[soil_moisture_c.time="2002-07-01T00:00:00Z"][soil_moisture_c.Longitude=-99.875], 21

soil_moisture_c.soil_moisture_c[soil_moisture_c.time="2002-07-02T00:00:00Z"][soil_moisture_c.Longitude=-99.875], 23

OPeNDAP Server Dataset Access Form

Action: [Get ASCII] [Get as NetCDF] [Binary (DAP) Object] [Show Help]

Data URL: http://hydro1.sci.gsfc.nasa.gov/opendap/hyrax/ncml/LPRM_AMSRE_D_SOILM3_timeSeries.

Global Attributes:
```
NC_GLOBAL.Conventions: CF-1.0
```

Variables: ☐ **Latitude**: Array of 32 bit Reals [Latitude = 0..719]
Latitude: [   ]
```
units: degrees_north
scale_factor: 1.00000000
add_offset: 0.00000000
long_name: Latitude
_CoordinateAxisType: Lat
```

☐ **Longitude**: Array of 32 bit Reals [Longitude = 0..1439]
Longitude: [   ]
```
units: degrees_east
scale_factor: 1.00000000
add_offset: 0.00000000
long_name: Longitude
_CoordinateAxisType: Lon
```

☐ **soil_moisture_c**: Grid of Array of 16 bit Integers [time = 0..3363][Longitude = 0..1439][Latitude = 0..719]
time: [   ] Longitude: [   ] Latitude: [   ]
```
soil_moisture_c.long_name: Volumetric Soil Moisture from C-band
soil_moisture_c.units: percent
soil_moisture_c.coordinates: Latitude Longitude
soil_moisture_c._FillValue: -32767
soil_moisture_c.scale_factor: 1.00000000
soil_moisture_c.add_offset: 0.00000000
```

☐ **soil_moisture_x**: Grid of Array of 16 bit Integers [time = 0..3363][Longitude = 0..1439][Latitude = 0..719]
time: [   ] Longitude: [   ] Latitude: [   ]
```
soil_moisture_x.long_name: Volumetric Soil Moisture from X-band
soil_moisture_x.units: percent
soil_moisture_x.coordinates: Latitude Longitude
soil_moisture_x._FillValue: -32767
soil_moisture_x.scale_factor: 1.00000000
soil_moisture_x.add_offset: 0.00000000
```

☐ **sm_c_error**: Grid of Array of 16 bit Integers [time = 0..3363][Longitude = 0..1439][Latitude = 0..719]
time: [   ] Longitude: [   ] Latitude: [   ]
```
sm_c_error.long_name: Uncertainty of Soil moisture in C-band
sm_c_error.units: percent
sm_c_error.coordinates: Latitude Longitude
sm_c_error._FillValue: -32767
sm_c_error.scale_factor: 0.00999999978
sm_c_error.add_offset: 0.00000000
```

☐ **sm_x_error**: Grid of Array of 16 bit Integers [time = 0..3363][Longitude = 0..1439][Latitude = 0..719]
time: [   ] Longitude: [   ] Latitude: [   ]
```
sm_x_error.long_name: Uncertainty of Soil moisture in X-band
sm_x_error.units: percent
sm_x_error.coordinates: Latitude Longitude
sm_x_error._FillValue: -32767
sm_x_error.scale_factor: 0.00999999978
sm_x_error.add_offset: 0.00000000
```

☐ **time**: Array of strings [time = 0..3363]
time: [   ]
```
_CoordinateAxisType: Time
```

Figure 25. NASA LPRM data retrieval site.
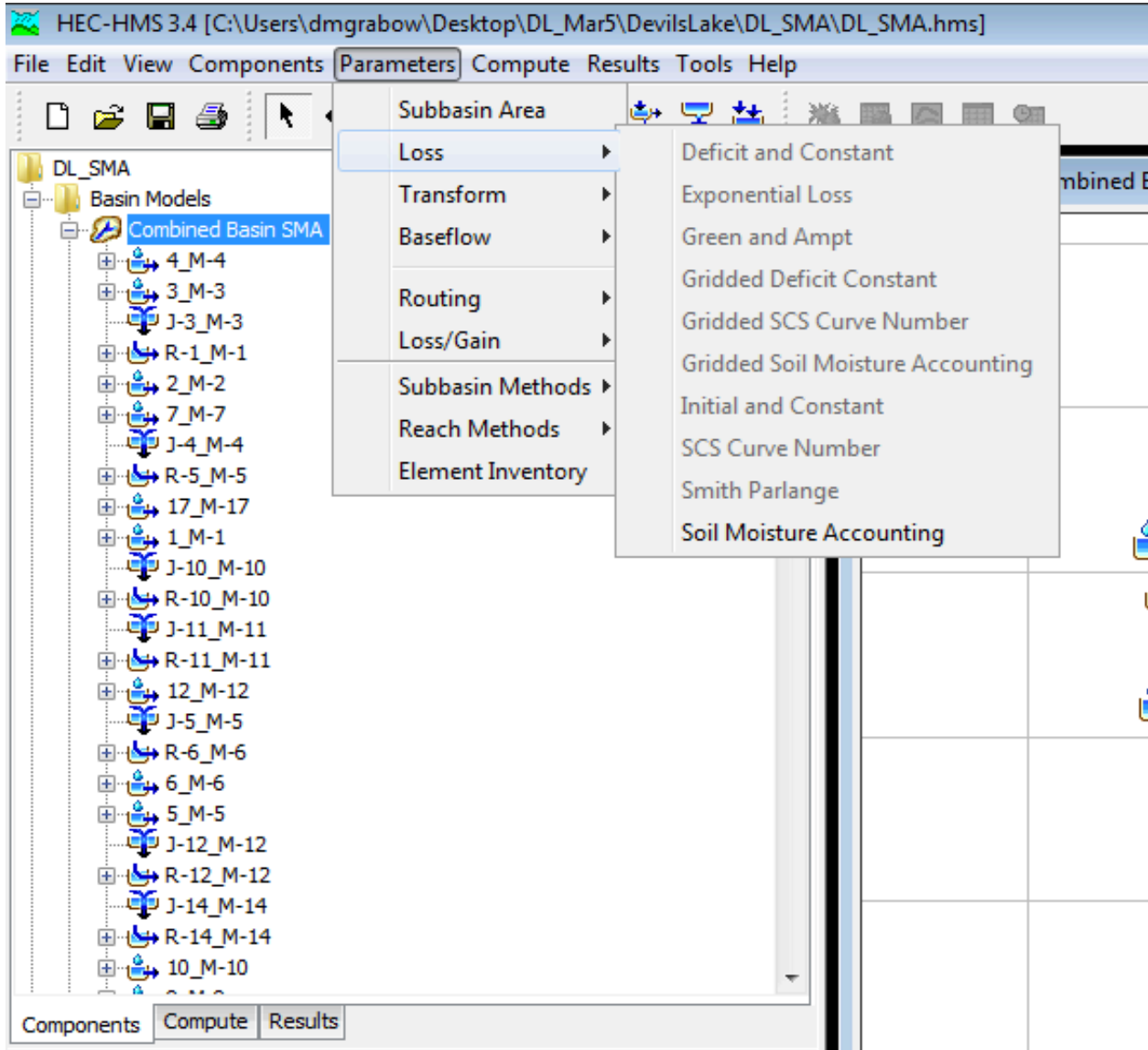(http://hydro1.sci.gsfc.nasa.gov/opendap/hyrax/ncml/LPRM_AMSRE_D_SOILM3_timeSeries.ncml.html)
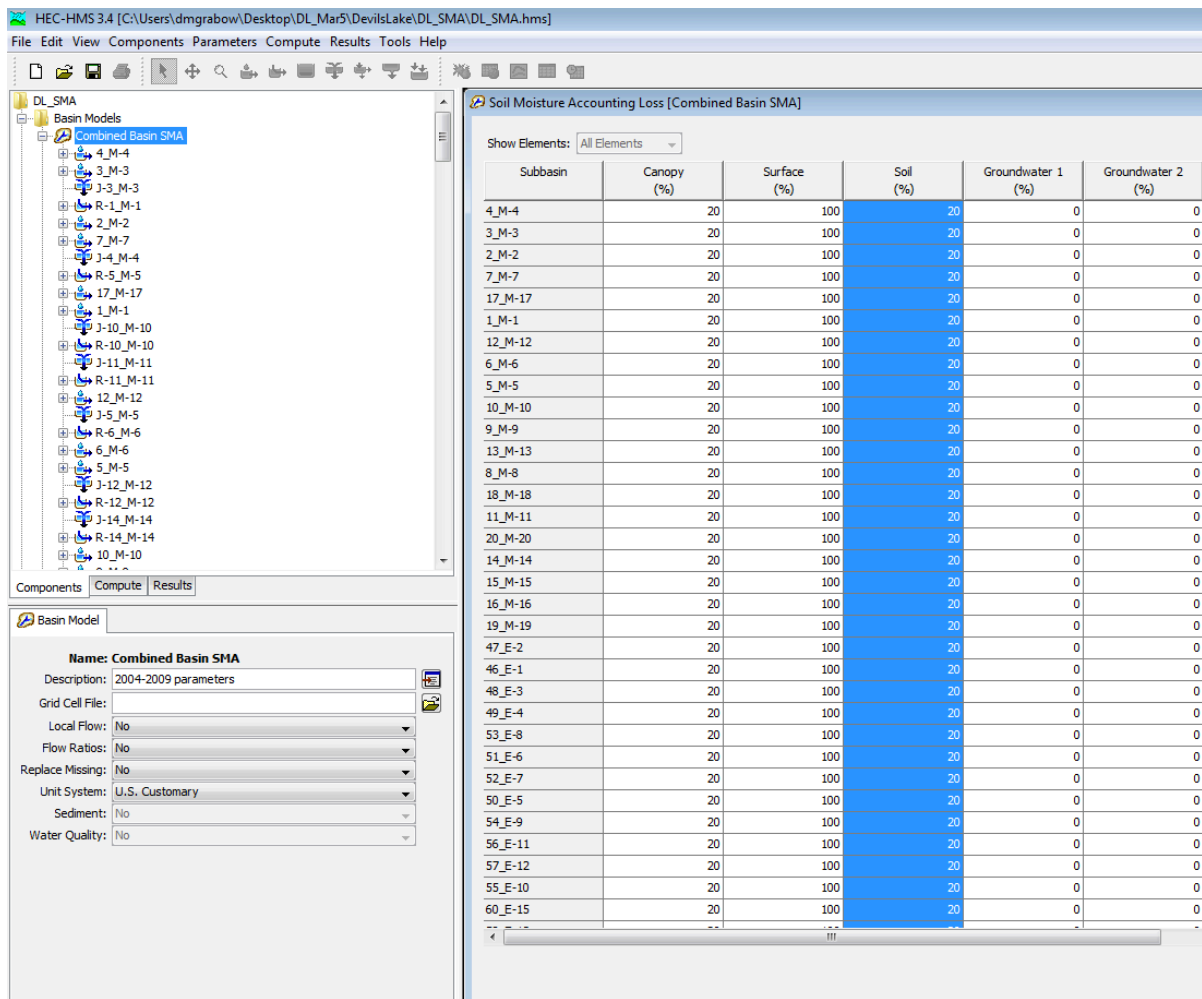
Figure 26. SMA data entry in HEC-HMS.

Figure 27. Soil moisture data entry location in HEC-HMS SMA parameters.

Figure 28. Snowmelt and evaporation parameters in HEC-HMS.

REFERENCES

Bennett, T.H. (1998). Development and application of a continuous soil moisture accounting algorithm for the Hydrologic Engineering Center Hydrologic Modeling System (HEC-HMS). MS thesis, Dept. of Civil and Environmental Engineering, University of California, Davis.

Brocca, L., Melone, F., Moramarco, T. Wagner, W., Naieme, V., Bartalis, Z., and Hasenauer, S. (2010). Improving runoff prediction through the assimilation of the ASCAT soil moisture product. Hydrology and Earth System Sciences Discussions, 7 (2010) 4113-4144.

Cosh, M. H., Jackson, T. J., Bindlish, R., Prueger, J.H. (2004). Watershed scale temporal and spatial stability of soil moisture and its role in validating satellite estimates. Remote Sensing of Environment, 92 (2004) 427-435.

de Jeu, R.A.M., Wagner, W., Holmes, T. R. H., Dolman, A. J., van de Giesen, N. C., Friesen, J. (2008). Global soil moisture patterns observed by space borne microwave radiometers and scatterometers. Survey of Geophysics, 28 (2008) 399-420.

Farnsworth and Thompson (1982). Mean Monthly, Seasonal, and Annual Pan Evaporation for the United States. NOAA Technical Report NWS 34. Office of Hydrology, National Weather Service, Washington D. C. December 1982, p. 45.

Gerla and Matheny (1996). Seasonal variability and simulation of groundwater flow in a prairie wetland. Hydrologic Processes, 10 (1996) 903-920.

Hafliger, K., Lim, Y. H. (2012). Flood Frequency Analysis of Devils lake under Current and Projected Future Climates Utilizing HEC Hydrologic Models, NASA Satellite Observations and Downscaled GCM Simulations. World Environmental and Water Resources Congress 2012: Crossing Boundaries © ASCE 2012.

Hassell, J. (2010). Devils Lake hydrologic model and prediction. (Master Thesis). University of North Dakota, Grand Forks, ND.

Hydrologic Engineering Center. (March 2000). Hydrologic Modeling System, HEC-HMS, Technical Reference Manual. Davis, CA: US Army Corps of Engineers.

Kirilenko, A. (2010). Climate Change Impact on Agriculture: Devils Lake basin. International Environmental Modelling and Software Society (iEMSs) 2010 International Congress on Environmental Modelling and Software Modelling for Environment's Sake, Fifth Biennial Meeting, Ontario, Canada.

Lim, Y.H., Hassell, J., Teng, W. (2010). Modeling Hydrologic Regime of a Terminal Lake Basin with GCM Down-scaled Scenarios. International Environmental Modelling and Software Society (iEMSs) 2010 International Congress on Environmental Modelling and Software Modelling for Environment's Sake, Fifth Biennial Meeting, Ontario, Canada.

Melesse, A. M., Nangia, V., Wang, X. (2006). Hydrology and Water Balance of Devils Lake Basin: Part 2 grid based spatial surface water balance modeling. Journal of Spatial Hydrology, 6 (2006) 133-144.

Miller, G. R., Baldocchi, D. D., Law, B. E., Meyers, T. (2007). An analysis of soil moisture dynamics using multi-year data from a network of micrometeorological observation sites. Advances in Water Resources, 30 (2007) 1065-1081.

Minet, J., Laloy, E., Lambot, S., Vanclooster, M. (2011) Effect of high-resolution spatial soil moisture variability on simulated runoff response using a distributed hydrologic model. Hydrology and Earth System Science, 15 (2011) 1323-1338.

Munna, H.S. (2012). Water level quantiles of Devils Lake under down-scaled GCM predictions using a coupled hydro-climatic model. (Master Thesis). University of North Dakota, Grand Forks, ND.

Nash, J.E. and Sutcliffe, J.V. (1970). River flow forecasting through conceptual models part 1 – A discussion of principles. Journal of Hydrology, 10 (1970) 282-290.

National Research Council (2007). Earth science and applications from space: National imperatives for the next decade and beyond, Committee on Earth Science and Applications from Space: A community Assessment and Strategy for the Future, pp. 437, Space Stud Board, Div. of Eng and Phys. Sci., Natl. Acad. Of Sci., Natl. Acad. Press, Washington, D. C.

Njoku, E. G. and Entekhabi, D. (1996). Passive microwave remote sensing of soil moisture. Journal of Hydrology, 184 (1996) 101-129.

Njoku, E., Ashcroft, P., and Li, L. (2005). Statistics and global survey of radio-frequency interference in AMSR-E land observations. IEEE Trans. Geosciences Remote Sensing, 43 (2005) 938-947.

North Dakota State Water Commission. (December, 2012). Devils Lake flood facts. Retrieved December 14, 2012, from http://www.swc.state.nd.us/4dlink9/4dcgi/GetContentPDF/PB-206/DLFactSheet.pdf

Owe, M., de Jeu, R., Holmes, T. (2008). Multi-sensor historical climatology of satellite-derived global land surface moisture. Journal of Geophysical Research, 113 (2008) F01002.

Raddatz, R. L. (2005) Moisture recycling on the Canadian Prairies for summer droughts and pluvials from 1997 to 2003. Agricultural and Forest Meteorology, 131 (2005) 13-26.

Raddatz, R. L. and Cummine, J. D. (2003). Inter-annual variability of moisture flux from the prairie agro-ecosystem: Impact of crop phenology on the seasonal pattern of tornado days. Boundary-Layer Meteorology, 106 (2003) 283-295.

Teng, W., de Jeu, R., Doraiswamy, P., Kempler, S., Mladenova, I., Shannon, H. (2010). Improving world agriculture supply and demand estimates by integrating NASA remote sensing soil moisture data into USDA world agricultural outlook board decision making environment. ASPRS Annual Conference, San Diego, CA. April 26-30, 2010.

U.S. Geological Survey. (n.d). Devils Lake Basin in North Dakota From http://nd.water.usgs.gov/devilslake/index.html

U.S. Army Corps of Engineers. (2010). Report of the Federal Interagency Devils Lake Working Group.

van der Camp and Hayashi (1998). The Groundwater Recharge Function of Small Wetlands in the Semi-Arid Northern Prairies. Great Plains Research 8 (Spring 1998):39-56.

van der Valk, A. G. (2005). Water-level fluctuations in North American prairie wetlands. Hydrobiologia 539 (2005) 171-188.

Vecchia, A. V. (2008). Climate Simulation and Flood Risk Analysis for 2008-2040 for Devils Lake, North Dakota. U.S. Geological Survey Scientific Investigations Report 2008-5011.

Wagner, W., Bloschl, G., Pampaloni, P., Calver, J. C., Bizzarri, B., Wigneron, J. P. (2007). Operational readiness of microwave remote sensing of soil moisture for hydrologic applications. Nordic Hydrology, 38 (2007) 1-20.

Wang, J.R., Schmugge, T.J. (1980). An empirical model for the complex dielectric permittivity of soil as a function of water content. IEEE Trans. Geoscience Remote Sensing. 18 (1980) 288-295.

Wang. L., Wen, J., Zhang, T., Zhao, Y., Tian, H., Shi, X., Wang, X., Liu, R., Zhang, J., Lu, S. (2009). Surface soil moisture estimates from AMSR-E observations over an arid area, Northwest China. Hydrology and Earth System Sciences Discussions, 6 (2009) 1055-1087.

Zhang, X. (2010). The Fate of Devils Lake: An Interwoven Aftermath of Agriculture and Climate Change. *2010 International Congress on Environmental Modelling and Software.* Ottawa: International Environmental Modelling and Software Society (iEMSs).